137 577 586 5070

PLACE IN RETURN BOX to remove this checkout from your record.
TO AVOID FINES return on or before date due.

DATE DUE	[redacted] STATE UNIVERSITY [redacted]	[redacted]ATE DUE
FEB 1 9 1999	[redacted]	
	[redacted]	

MSU Is An Affirmative Action/Equal Opportunity Institution

Order Number 1336045

Experimental study on some property effects and one-dimensional modeling of the cure and residual stress for thermal and electromagnetic curing of epoxy resin

Singer, Stephen Mark, M.S.

Michigan State University, 1988

U·M·I
300 N. Zeeb Rd.
Ann Arbor, MI 48106

EXPERIMENTAL STUDY ON SOME PROPERTY EFFECTS AND ONE-DIMENSIONAL MODELING OF THE CURE AND RESIDUAL STRESS FOR THERMAL AND ELECTROMAGNETIC CURING OF EPOXY RESIN

by

Stephen Mark Singer

A THESIS

Submitted to
Michigan State University
in partial fulfillment of the requirements
for the degree of

MASTER OF SCIENCE

Department of Chemical Engineering

1988

ABSTRACT

EXPERIMENTAL STUDY ON SOME PROPERTY EFFECTS AND ONE-DIMENSIONAL MODELING OF THE CURE AND RESIDUAL STRESS FOR THERMAL AND ELECTROMAGNETIC CURING OF EPOXY RESIN

By

Stephen Mark Singer

An experimental study on the property effects and modeling of the cure and residual stress simulation for thermal and electromagnetic processing of the DER 332 / DDS epoxy resin has been performed. The two physical properties investigated in this study were the thermal expansion coefficient and the glass transition temperature. The two mechanical properties studied were the Young's modulus and the tensile strength. All of these properties were studied as a function of the type of processing as well as the extent of cure. A simulation which modeled the thermal and electromagnetic curing of the epoxy resin system using kinetic expressions and heat transfer equations has been developed. Residual stresses resulting from the non-uniform cooling of a non-uniformally cured material were simulated. The residual stress simulation incorporated the experimental values obtained from the physical and mechanical property testing with thermal and electromagnetic cure simulation.

ACKNOWLEDGEMENT

This project is sponsored by the URI grant on thick section composites from the University of Illinois, as well as funding provided through the State of Michigan through a REED grant. I would like to thank Dr. Martin Hawley for his support and guidance during this study, and thank Dr. Jinder Jow for his many discussions and valuable suggestions during this study. Finally, I would like to thank my parents for their love and support through the years.

TABLE OF CONTENTS

LIST OF TABLES

LIST OF FIGURES

INTRODUCTION

Epoxy resins were first synthesized in the late 1930's and developed commercially for industrial uses in the early 1940's. Epoxy resins are characterized by an epoxide group which can be reacted with curing agents or catalytically polymerized to form a cross-linked polymeric structure. Cured epoxy resins have good mechanical and electrical properties as well as excellent heat and chemical resistance. The properties attained by a cured epoxy resin are largely dependent on the curing system used to convert it to a cross-linked polymer. Epoxy resins have applications in five basic areas. These areas include coatings, electrical and electronic insulation, adhesives, construction, and composites. Throughout the last twenty years, epoxy resins have been studied extensively as the matrix material in fiber reinforced composite materials. This particular study focuses in on the processing and the resultant properties of the DER 332 / DDS epoxy resin system.

Typically, epoxy resins have been thermally processed. Microwave energy, which is an alternative method to process epoxy resins, is being investigated in this study. Areas to be covered in this study include the comparison of certain

physical and mechanical properties resulting from thermal and electromagnetic processing, and the development of a cure simulation and a residual stress model for both thermal and electromagnetic processing.

The primary objectives in the study include experimentally determining the glass transition temperature, the thermal expansion coefficient, the Young's modulus, and the tensile strength of the cured epoxy resin resulting from both thermal and electromagnetic processing as well as developing a model which simulates the thermal and electromagnetic curing of the DER 332 / DDS epoxy resin from kinetic and heat transfer expressions. Residual stress profiles for the simulated cures were also determined. The curing of thick section epoxy resins is non-uniform due to large temperature gradients which occur in the material. The residual stresses develop due to the cooldown of the non-uniformally cured material. These stresses will be evaluated at different curing temperatures and thicknesses in a thermal environment, and at different power densities and thicknesses in an electromagnetic environment.

Three steps are involved in effectively simulating the residual stresses in a material. The first step is to determine certain physical and mechanical properties as a function of the extent of cure for both thermal and

electromagnetic processing. The second step is simulate the thermal and electromagnetic curing of an epoxy resin sample. The final step, the residual stress simulation, incorporates the physical and mechanical properties and the cure simulations.

BACKGROUND AND LITERATURE REVIEW

Curing Processes

Epoxy resins are classified to be thermoset materials. A thermoset is defined to be a polymeric material which can be formed by the application of heat and pressure, but, as a result of chemical reaction, permanently crosslinks and cannot be reformed under further application of heat and pressure (1).

Epoxy resins, when unreacted, are typically a linear, polymer chain. These linear polymer chains form a cross-linked polymer when the epoxy resin and the curing agent reacts. There are several key steps that thermosetting materials follow to become cross-linked systems. Prime (2), describes two material stages during curing. As the resin cures, a sudden irreversible change from a viscous liquid to an elastic gel occurs. This borderline stage is called the gel point. When a polymer reaches the gel point, it is no longer processable. The viscosity of the mixture approaches infinity as the polymeric mass becomes a solid. Prime notes that gelation usually occurs when the reaction is typically 50 - 80 percent completed (2).

Another phenomenon that may occur is the vitrification

process. This process is the transformation of a viscous liquid or an elastic gel to the glassy state. The transformation to the glassy state is when the glass transition temperature of the material reaches the curing temperature at which the material is placed. The glass transition temperature is defined to be the temperature at which the material changes to a soft, rubbery, state from a hard, brittle, glassy, state. Prime adds that in order to achieve a complete cure and develop ultimate properties, the vitrification process must be avoided (2).

The glass transition temperature of a material increases as the amount of cross-linking increases (3). A theoretical equation which relates the glass transition temperature to the extent of cure was developed by DiBennedetto and is: (3,4)

$$\frac{T_g - T_{go}}{T_{go}} = \frac{[\, E_x/E_m - F_x/F_m \,] * X}{[\, 1 - (\, 1 - F_x/F_m \,) * X \,]}$$

where X = extent of cure
T_g = glass transition temperature
T_{go} = glass transition temperature of unreacted material
E_x/E_m = ratio of lattice energies for cross-linked and uncross-linked polymer
F_x/F_m = ratio of segmental mobilities for cross-linked and uncross-linked polymers

Bidstrup, et al. (4), used the DiBennedetto equation to relate the glass transition temperature to the extent of cure. The values that are estimated for the DER 332 / DDS

system for the E_x/E_m, the F_x/F_m, and the T_{go} are 0.30, 0.18, and 293 °C, respectively (4). There is good agreement between the theoretical equation using these values and experimental data they obtained using the Differential Scanning Calorimeter.

Generally, the glass transition temperature of a material will not go much higher than the curing temperature or the temperature at which the material was formed. Addabo and Williams (5) note that at the glass transition temperature, the conversion and temperature levels are such that the network segments become almost immobilized, and the chemical reaction becomes stopped for practical purposes.

Rate Kinetics

Understanding and knowing the kinetics of an epoxy-amine reaction is of primary importance. Kinetic expressions can be used in the modeling of temperature profiles during the course of a reaction. Rate constants and activation energies from the kinetic expressions are two parameters which yield insight into how the reaction proceeds. Rate kinetics for thermoset materials can be determined a number of ways. One of the most popular methods is to use Differential Scanning Calorimetry (DSC). Differential Scanning Calorimetry is the measurement of the difference in heat flow of a sample and a reference pan

while the sample is maintained in a controlled temperature environment.

Barton (6) discusses instrumental and experimental aspects as well as methods of analyzing the kinetic data obtained through the DSC. DSC can provide data on overall reaction kinetics with relative speed and ease. DSC can also provide measurements of a glass transition temperature which will give an indication of the degree of cross-linking of an epoxy resin.

A major assumption in DSC work is that the heat flow relative to the baseline is proportional to the reaction rate (6). A second assumption in DSC kinetics is that the temperature gradient through the sample is negligible. Controlling the sample size and shape, as well as the operating conditions of the DSC are necessary to alleviate the effects of the assumptions.

Numerous investigators have studied reaction kinetics of thermoset materials through the DSC (2,6-10). Sichina (7), has developed a procedure to determine the proper methods and cycles to correctly analyze the reaction kinetics. Rate mechanisms for thermoset curing can be divided into two categories (2): N_{th} order kinetics and autocatalyzed kinetics. A n_{th} order system has the rate of conversion proportional to the concentration of the

unreacted material. The maximum rate of reaction in n_{th} order kinetics occurs at the beginning when all of the reactants are present. An expression which describes the rate of reaction of n_{th} order kinetics is:

$$\frac{\delta X}{\delta t} = K * (1-X)^n$$

where X = the extent of cure
K = a rate constant
n = the order of the reaction

Autocatalyzed kinetic reaction systems are characterized by the formation of an intermediate group which accelerates the reaction. In autocatalyzed rate kinetics, the rate of reaction is typically a maximum when the extent of cure is approximately 30 - 40 percent. An expression which describes autocatalyzed rate kinetics is:

$$\frac{\delta X}{\delta t} = K * X^m * (1-X)^n$$

where X = extent of cure
K = a rate constant
m = the order of the reaction
n = the order of the reaction

The rate constant, K, found in both expressions, is generally of the Arrhenius form:

$$K = A * \exp(-E/(R * T))$$

where A = a constant
E = the activation energy
R = the gas constant
T = the temperature

Mijovic (8), studied the kinetics of a tetrafunctional epoxy resin with an aromatic diamine. He found that the reaction rate passes through a maximum when the extent of cure was at 30 percent, and then decreased as a function of cure time. He also noted that when there is a decrease in cure temperature, the reaction rate decreased, and the reaction shifted to a longer curing time. These observations are characteristic of an autocatalyzed system.

Moroni et al. (9), determined the curing kinetics of a bifunctional epoxy resin and an arcmatic diamine in a recent study. They reported that there were several different mechanisms which occur during the cure of an epoxy formulation. Moroni used thermal analysis to distinguish the different mechanisms. They also note that as the autocatalytic nature of the reaction decreases at lower curing temperatures, the distinction between the primary and subsequent reactions become less pronounced.

Stoichiometry plays an important part in reaction kinetics. Several studies evaluate the effect of the

concentration of the curing agent on the reaction rate with conflicting results. Hagnauer et al. (10), studied the effects of impurities and stoichiometric changes on the curing kinetics of thermoset materials. The major conclusions were that impurities increase the reaction rate and that increasing the concentration ratio between the curing agent (amine) and epoxy decreases the reaction rate. The increased concentration also provided for a higher degree of cross-linking. Mijovic (8), in a more recent study, also agrees that increased stoichiometry provides for a higher degree of cross-linking. However, Mijovic concludes that a higher curing agent concentration increased the reaction rate. Moroni et al. (9), add that a departure from the stoichiometric ratio increases the reaction rate.

Thermal Processing

Epoxy resins and fiber reinforced composites have typically been processed in a thermal environment. The heating mechanism for a sample placed in a thermal environment is through its boundaries. The combination of heat, pressure and a vacuum are used in the thermal processing of materials. The processing cycle is dependent on the materials involved and the resultant material properties desired.

Typical thermal processing begins by placing the sample in a vacuum bag. The sample is then placed in an autoclave, and a vacuum is generally drawn in the bag. The purpose of the vacuum is to begin consolidation of the plies or layers, and to remove excess air and moisture entrapped in the resin and the bag. Air or moisture entrapped in the sample can cause voids or holes, which can decrease the performance of the material. The temperature in the autoclave is increased to a preset value, and an external pressure is applied to the sample. The increased temperature will begin the chemical reaction process, and the external pressure applied will consolidate the plies even further, along with driving out excess resin in the sample. The autoclave is maintained at these conditions for the remainder of the specified curing cycle.

Electromagnetic Processing

Using microwave energy to cure thermoset epoxy resins has become increasingly popular in the last decade. Microwave energy has been applied to the processing of thermosetting resins in single mode microwave ovens (11,12), multimode microwave ovens (13,14), and wave guides (15,16). Indications from these experiments suggests that there is an acceleration of the curing process when using microwave energy.

Microwave energy is defined as an electric field oscillating at the rate of 100 to 300,000 million cycles per second. When a dielectric material is placed in this field, the molecules attempt to move and align themselves with the oscillating field. The alignment ability of the polar functional groups within the molecules is defined as the dielectric constant. The polar functional groups in the reacting molecules try to align themselves with the oscillating electric field. A molecular "friction" between the functional groups takes place as this happens. The friction between the molecules results in a temperature increase in the material. The increase in temperature initiates the curing process. The mobility and the population of the polar groups is defined as the dielectric loss factor.

An advantage of the electromagnetic heating process is that thermal heat conduction through the material is not necessary. The electric field frequency, the electric field strength, and the dielectric behavior of the material are all important considerations in the curing of epoxy resins using microwave applicators. The power absorbed by the material is the product of the electric field frequency, the dielectric loss factor, and the square of the electric field strength. Strand describes a fast microwave heating equation which relates the change of temperature in a dielectric material to the power absorbed in the material:

$$\rho * C_v * \frac{\delta T}{\delta t} = P_w$$

where ρ = the density of the material
C_p = the heat capacity of the material
T^p = the temperature
P_w = the power absorbed in the material

The power absorbed in the material can be related to electromagnetic parameters and the dielectric loss factor:

$$P_w = \frac{1}{2} * \omega * \epsilon'' * [E]^2$$

where ω = the frequency of the microwave energy
ϵ'' = the dielectric loss factor of the material
E = the energy of the emitter

Wilson and Salerno (17), also derive a mathematical relation for the rate of electromagnetic heating of epoxy resin in terms of the electric field parameters, as well parameters dependent on the material. They note that a certain temperature, the exothermic reaction becomes dominant, and that the temperature of the sample increases dramatically. They suggested that this sudden increase in temperature can result in the boiling of the resin.

Lewis et al. (12), indicated that there is a reduction in processing time is due to a significant acceleration in the curing reaction when using microwave energy to process epoxy resins. Also, they have found that the flexural modulus and fracture toughness properties of a

electromagnetically processed sample were comparable to a thermally processed sample.

Physical Properties

Mijovic and Wang (18), studied the effect of autoclave processing on the physical properties of an epoxy resin system. They found that the density of their epoxy resin system increased a total of 2 percent due to the effect of the bridging of molecules from cross-linking reactions. They also found that the density was a slight function of the extent of cure until the extent of cure reached 50 percent. The density then remained constant until the extent of cure reached 100 percent.

Shimbo et al. (19), describe the density change of the curing process in four different stages. The first stage is the decrease of the density by increasing the temperature of the resin to the curing temperature. The second step is the shrinkage by reaction curing at the curing temperature. The third phase is the shrinkage by cooling from the reaction temperature to the glass transition temperature. The last step is the cooling from the glass transition temperature of the material to room temperature. These last two cooling steps have different slopes because the thermal expansion coefficient is higher in the range between the curing and glass transition temperature than in the range between the

glass transition temperature and the room temperature.

Nielsen (3), indicates that cross-linking increases the thermal conductivity of a thermoset material slightly. The effect is not significant at high degrees of cross-linking. An explanation for this effect is that the flow of heat is greater along covalently bonded chains than across chains bonded with weak Van der Waals forces (3). Mijovic and Wang (18), in a more recent study, agreed that increasing the extent of cure increased the thermal conductivity. They also found that an increase in temperature increased the thermal conductivity.

Mijovic and Wang (18), found that the heat capacity of the resin increases slightly as a function of the curing temperature and cure time. They also noted that the heat capacity decreased as the extent of cure increases.

Mechanical Properties

The mechanical properties of an epoxy resin system are determined by the curing agent and the processing cycle (20). Epoxy resins can be formulated to yield a variety of properties ranging from soft, flexible, products to hard, tough, materials (21). Gupta et al. (22), add that the mechanical properties depend on chemical structure, molecular architecture, cross-link density and free volume.

Free volume is defined as being the difference between the measured volume and the occupied volume of a polymer. The occupied volume is the volume occupied by the mass of the molecule plus the volume it occupies due to thermal vibrations of the molecule (23). Morgan (24), suggests that the mechanical properties exhibit a free volume dependence as a function of thermal history. A decrease in free volume results in a more brittle mechanical response. Below a specific temperature, the glassy state mobility is too small to allow for any changes in the free volume. Morgan also notes that rapid cooling from above produces a glass with a larger free volume.

The tensile strength is representative of the material's strength because the whole cross-section of the material is subjected to a uniform stress. Failure of a specimen will occur where the largest flaw is located (22). Gupta et al. (22), studied the effects of processing on the mechanical properties on a bifunctional epoxy resin and an aromatic diamine. They noted that a change in tensile strength can indicate a change in structure, cross-link density, and intermolecular packing. Nielsen (3), and Gupta et al. (22), note that the tensile strength of an thermoset first increases with cross-linking, and then progressively decreases. Theoretically, one would expect the tensile strength to increase with cross-linking because weak Van der Waals bonds are being replaced with strong,

covalent bonds. The decrease in tensile strength may be due to the submicroscopic cracks developing from internal stresses which result from shrinkage or thermal changes during the cooling of the material (3).

The elastic modulus of a material is dependent on the molecular arrangement because the resistance to deformation arises from the intermolecular forces (22). Enns and Gilliham (25), point out that the modulus of a thermoset material decreases as the extent of cure increases. Gupta et al. (22), found similarity between their modulus data and their density data. They suggested that the intermolecular packing was a predominant factor when the material was tested at room temperature. They also found that a material with a high glass transition temperature had the lowest modulus suggesting that the intermolecular packing is large. A sample with a high glass transition temperature has more free volume trapped in it when cooled to room temperature.

Post curing a material has significant effects on the mechanical properties of epoxy resins. Gupta et al. (22), found that the tensile strength decreases on postcuring. This indicates that the increase in free volume plays a substantial role when compared to the increase in cross-link density.

Hagnauer et al. (10), note that post-curing decreases the compressive strength and stiffness of the material. The decrease in stiffness may result from a decrease in density which tends to occur in post-curing. In order to effectively post-cure a material, the temperature must be above the glass transition temperature of the material. The thermal expansion coefficient is higher during the heating to the post-cure temperature, than during the subsequent cooling to room temperature. This accounts for the change in density of the material (10).

Several studies have been performed regarding the effect of stoichiometry on the mechanical properties of epoxy resins. Hagnauer et al. (10), studied the effects of impurities and the stochiometric changes on the mechanical properties of thermoset materials. He noted that changes in the stoichiometric ratio or the addition of impurities had no significant effect on the mechanical properties.

Gupta et al. (22), noted that reaction stoichiometry has a considerable effect on the resultant mechanical properties. The elastic modulus at room temperature for their particular epoxy resin system drops to a minimum at the stoichiometric mixture, and then increases to values some 20 percent higher as the concentration of the curing agent departs from the reaction stoichiometry. They noted that the tensile strength at room temperature increases

rapidly to the stoichiometric mixture, and then slowly increases as excess curing agent is added. They also found that the elongation-to-break at room temperature increases to a maximum at the stoichiometric mixture and then decreases as the concentration of the curing agent departs from the stoichiometry. Morgan (24), agrees that the maximum elongation-to-break occurs at the proper reaction stoichiometry.

Modeling

Modeling the curing of an epoxy resin system has become increasingly important and popular in the last several years. Optimum properties, as well reduced processing times can be the result of a judicious study. The control of a curing process is important in the case of structural materials which are designed to satisfy certain design considerations. Simulating the curing will give temperature, extent of cure, viscosity, pressure, void, and residual stress profiles.

Several studies have been undertaken during the last few years (18,26,27). Cure simulation starts with a complete material and energy balance over the entire system. An equation which describes the material balance for the system is:

$$\frac{dX}{dt} = \frac{-r}{C_{ao}}$$

where X = extent of cure
t = time
r = rate of reaction
C_{ao} = initial concentration of limiting reactant

An equation which describes the rate of heat generated per unit volume from the chemical reaction is:

$$\frac{dH}{dt} = \frac{dX}{dt} * H_{rxn}$$

where H_{rxn} = heat of reaction per unit volume

An equation which describes the one-dimensional energy balance in the x-direction is:

$$\rho * C_v * \frac{\delta T}{\delta t} = \frac{\delta}{\delta x}\left\{ \kappa \frac{\delta T}{\delta x} \right\} + \rho * \frac{dH}{dt}$$

where T = temperature
ρ = density
C_v = heat capacity
κ = thermal conductivity

The term on the left hand side of the equation is the amount of energy accumulated in the system per unit time. The first term on the right hand side is the net amount of energy entering or leaving the system in the x-direction through conduction. The second term on the right hand side is the amount of energy generated by the exothermic reaction. A simplifying assumption that energy transfer by convection is neglected because resin flow within the system

is small. The initial conditions for the system are:

$$T = T_i \ (x) \quad \text{for } 0 < x < L$$

$$X = 0 \quad \text{for } t < 0$$

where X = extent of cure
T_i = the initial temperature of the resin
0 and L represent the boundaries of the system.

The boundary conditions for the system are:

$$T = T_{bound} \quad \text{at } x = 0 \text{ and } t > 0$$
$$T = T_{bound} \quad \text{at } x = L \text{ and } t > 0$$

where T_{bound} = the oven temperature.

Mijovic and Wang (18), as well as Loos and Springer (26), incorporated other models such as resin flow and pressure distribution into the heat transfer and kinetics model to obtain a more comprehensive simulation. Conversion of the models, as well as the initial and boundary conditions into computer code is necessary due to the numerous calculations involved.

Mijovic and Wang (18), through their simulation program, studied the temperature profiles during the curing of an epoxy resin composite. They note that as the thickness of a composite increases, the temperature gradient between the boundary and the center also increases. For a 32 ply composite, the simulated temperature during curing in the center is only 10 °C greater than the boundary

temperature. However, for a 128 ply composite, the center temperature is approximately 90 °C above the boundary temperature. With a strong temperature gradient through the sample, the curing of the material can be non-uniform. The non-uniformity in temperature and cure distribution can have significant effects on the residual stress profiles of the material. Mijovic and Wang (18) also add that there is quite a bit of thermal lag when curing a thicker specimen when compared to a thin specimen. This lag increases the processing time to achieve a proper cure.

Kardos, etal (27) modeled the formation, growth and transport of voids during composite laminate processing. They noted that voids can be formed by entrapment of air mechanically. The entrapment of air can be caused by one of the several following reasons:

1. Entrained gas bubbles from the resin mixing operation.
2. Bridging voids from large particles, broken fibers or contaminants.
3. Air pockets or wrinkles in prepeg sheets created during ply stacking.

Depending on the materials being used, water vapor can diffuse into these air bubbles, and under certain temperature and constant volume conditions, the total pressure in the bubble can rise. This results in growth of the void.

Loos and Springer (26) conclude that the specification

and selection of the curing cycle is very important. Three points to consider in determining the cure cycle are:

1. The temperature at any location does not exceed a preset maximum.
2. The resin is cured uniformly, and the degree of cure is a specified value throughout.
3. The curing of the resin is done in the shortest possible time.

Residual Stress

A thermoset material can develop residual stresses from a processing cycle (19). These stresses are due to shrinkage or contraction of the resin which results from cooling down from a glass transition temperature to a room temperature.

Shimbo et al. (19), investigated the mechanism of internal stress and shrinkage and the relationship between these properties and the chemical structure of the epoxy resin. They noted that an increase of shrinkage an internal stress occurred as the concentration of network chains and glass transition temperature of the system increased. They found that the shrinkage in the glassy region increased as a constant ratio with decreasing ambient temperature. Internal stress was absent in the rubbery region where $T > T_g$. However, the internal stress increased dramatically with decreasing ambient temperature in the glassy region ($T < T_g$). They found that a linear relationship existed between the internal stress and the

shrinkage when in the glassy region. They concluded that the shrinkages in the glassy region were converted directly to internal stress because the mobility of the network segments are restricted in the glassy region. They also determined that the internal stress is expected to decrease with an increase in the chain length of the epoxy resins.

Srivista and White (28) determined the curing stresses of an epoxy resin cured at different isothermal temperatures. They used a layer removal technique to experimentally determine the stresses as a function of location. This method consists of removing thin uniform layers from a parallel sided epoxy resin sheet. The imbalance of stresses will cause a curvature in the sheet. The curvature was measured by the use of lasers, and stresses were calculated from an equation involving the material properties of the resin. They found that there were tensile stresses were found to be in the interior, while compressive stresses were found near to the surface in all samples tested. Compressive stresses at the exterior may be of some benefit because they tend to inhibit crack propagation from a surface flaw or defect. Tensile stresses in the interior will add to an externally applied stress. This will reduce the load required to promote fracture in that particular region.

Materials cured at 80 °C had low stresses present with

a maximum compressive stress close to .5 MPa, and a tensile stress of .25 MPa. Higher stresses were found in samples that were cured at higher temperature. Compressive stresses were in the range of 1 MPa, while tensile stresses were in the range of .6 MPa for a sample cured at 135 °C. They concluded that samples that are cured at lower temperatures will have lower residual stresses (28).

Igarashi et al. (29), studied the contractive stresses of an epoxy-amine system during isothermal curing by photoelastic and bimetallic methods. Polarized incident light is directed through a transparent and optically isotropic material in the photoelastic method of determining residual stresses. The stresses occuring in the material decompose the transmitted light into two components of different velocities which are polarized in the direction of the principal axes of the stresses (29). An equation relates the fringe order to the principal stress difference in the sample (29).

In the bimetallic method. a thin steel strip is coated with the resin and is placed on two knife edges. The deflection of the strip caused by the contraction of the resin is measured. The contractive stress is calculated from equations using the material properties and the moment of inertia of the bending strip (29).

Igarashi et al. (29), observed the contractive stress only after the gelation of the resin. The maximum value of the stress that occurred was 4.6 MPa by the photoelastic method. A value of .1 MPa was obtained through the bimetallic method. They concluded that the occurrence of the stresses is subject to the behavior of the elastic modulus associated with the gelation of the resin.

Tsai and Hahn (30) suggest that most of the cross-linking that takes place at the cure temperature. However, epoxy resin may be viscous enough to allow for complete relaxation of stresses. The cure temperature can serve as the stress free temperature as long as most of the curing takes place at that temperature. They also present the calculations necessary to determine the stresses in a composite laminate.

There are three steps which describe the mechanism for generating residual stress in samples. The first step is the cooldown of the sample from an elevated temperature to the glass transition temperature of the material. Stresses begin to originate when the temperature of the material is equal to the glass transition temperature of the material. An explanation for this is that the network segments become rigid, and relaxation of the segments is not possible. When the temperature of the material is above the glass transition temperature, relaxation of the network segments

is possible and stresses cannot originate.

The second step is where the surface of the sample is quenched to ambient temperature. Since the thermal conductivity of the resin is small, the internal region (center) does not undergo any change.

The third step is the gradual cooldown of the entire sample to the ambient temperature. Since the surface and the internal region constrain each other, the external layer enters a compressive state and the center region enters into a tensile state.

EXPERIMENTAL STUDY ON SOME PROPERTY EFFECTS FOR THERMAL AND MICROWAVE CURING OF THE DER 332 /DDS EPOXY RESIN

Sample Preparation

Two chemicals are used to prepare the epoxy resin matrix material. The resin used is DER 332, and is manufactured by Dow Chemical Corporation, Midland, Michigan. Shown in Figure 1 is a Diglycidyl Ether of Bisphenol A (DGEBA) type resin. DER 332 is a DGEBA type resin, and there are no repeating units in its structure: therefore n = 0 for this particular resin. The chemical structure of DER 332 is shown in Figure 2. The molecular weight of DER 332 is 336 grams per mole.

The curing agent used is Diamino-diphenylsulfone (DDS), and it is manufactured by the Aldrich Chemical Company in Milwaukee, Wisconsin. The chemical structure of DDS is shown in Figure 3. The molecular weight of DDS is 248 grams per mole.

A stoichiometric mixture was used throughout this study. A stoichiometric mixture consists of 36 grams of DDS to 100 grams of DER 332. The DDS was added to the epoxy resin slowly, and at approximately 130 °C, the DDS will dissolve into solution. The solution was stirred until all of the DDS disappeared. The resulting mixture was placed in

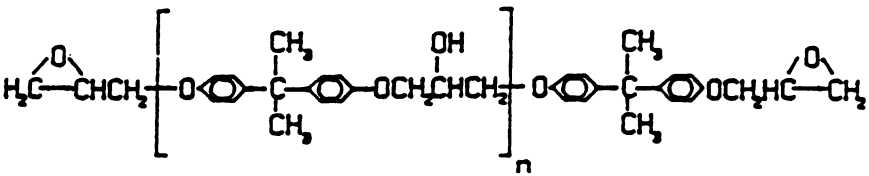

Figure 1). Chemical structure of DiGlycidyl Ether of Bisphenol A (DGEBA) resin.

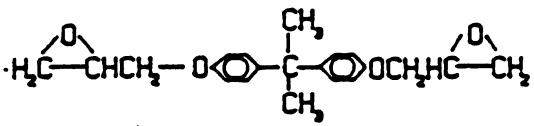

Figure 2). Chemical structure of DER 332 epoxy resin.

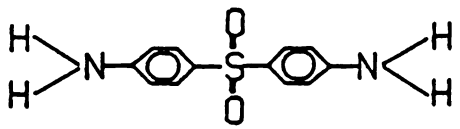

Figure 3). Chemical structure of Diamino-diphenyl sulfone.

a vacuum oven at 80 °C. The mixture was de-gassed for a period of 30 minutes under 20 - 25 inches of mercury. The purpose of this step is to eliminate any dissolved or trapped air in the liquid. When cured, any residual air will create voids, and thus will decrease the performance of the material. After the de-gassing procedure, the resin was either used immediately, or was frozen at -10 °C.

Samples for mechanical or physical property testing were cast in silicon rubber molds. The silicon rubber used for the molds was RTV 664, and is manufactured by General Electric, Waterford, New York. To improve the "flowability" of the resin in the mold, both the resin and the mold were heated prior to the casting. The mold was then placed in either a thermal oven or in an electromagnetic cavity and then cured to the appropriate specifications.

Two different sample shapes were used for the physical and mechanical property testing. For the thermal expansion experiments, the sample that was used is shown in Figure 4. The sample that was used for the mechanical testing is shown in Figure 5. These sample shapes were chosen because they were small enough to minimize temperature gradients during the curing cycle. Temperature gradients during the curing of an epoxy resin can cause a non-uniformally cured sample. The dog-bone sample used for the mechanical testing was ideally suited for electromagnetic processing because of its

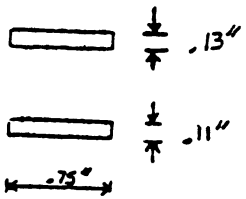

Figure 4). Description of sample used for thermal expansion tests.

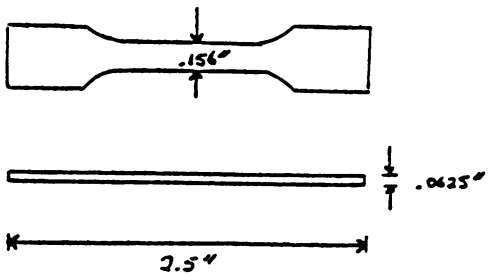

Figure 5). Description of sample used for mechanical testing.

EXPERIMENTAL PROCEDURES

Differential Scanning Calorimetry

The method used to determine the heat of reaction, the extent of cure, the glass transition temperature, and the reaction kinetics of the DER 332 / DDS epoxy resin was by the use of the Differential Scanning Calorimeter (DSC). The DSC is used to measure the heat flow into or out of a sample placed in its cell as it is exposed to a controlled temperature profile. Samples ranging from 10 to 15 milligrams were set into an aluminum pan and then hermetically sealed before being placed into the DSC cell. A reference pan is also prepared and placed into the DSC cell. By using a reference pan, the effects of the heat capacity of the aluminum are compensated. The primary operating environments ofthe DSC are under a isothermal temperature condition and under a ramping temperature condition.

When the total heat flow out of the sample is integrated, the heat of reaction (exotherm) between the reactants can be determined. The maximum heat of reaction for the DER 332 / DDS system is dependent on the operating conditions of the DSC. A sample is determined to be fully cured when there is no change in the heat flow. When a sample is partially cured, it will have a residual heat of

reaction less than the maximum exotherm for those specified conditions. The extent of cure is defined to be:

$$\text{Extent of Cure} = \frac{H_{rxn}\ \text{maximum} - H_{rxn}\ \text{sample}}{H_{rxn}\ \text{maximum}}$$

The residual heat of reaction of a sample that is partially cured is determined by a ramping temperature method. Under these operating conditions, the temperature of the sample that is placed in the DSC cell is increased at a rate of 5 °C or 10 °C per minute. The maximum exotherms attained by curing fresh epoxy resin at a ramping rate of 5 °C and 10 °C per minute are 372 and 330 joules per gram, respectively. These ramping temperature runs begin at room temperature and are taken to approximately 350 °C. The temperature at the end of the ramping DSC run is much higher than the temperature needed to cure the material. This extra temperature is needed to facilitate complete conversion of reactants into products. A typical DSC scan is shown in Figure 39, Appendix A. This particular sample was ramped at 10 °C per minute to 350 °C. When the total heat flow was integrated, the resulting exotherm was 124 joules per gram. The extent of cure for this particular sample was 62 percent.

The first method used to determine the glass transition temperature of the thermally and combination cured epoxy resin sample. was by the use of a a Differential Scanning

Calorimeter operated at a 10 °C per minute ramping temperature from room temperature to 350 °C . As the temperature of the sample is raised, the DSC is able to record a noticeable change in the heat flow when the sample changes states. A typical glass transition curve is shown in Figure 40, Appendix A. Three temperatures are indicated by the analysis. These temperatures correspond to the onset, inflection, and final glass transition temperature. The temperature that is usually reported in the literature is the inflection temperature.

Thermal Expansion

Thermal expansion measurements for the DER 332 / DDS epoxy resin samples were performed in a DuPont Thermal Mechanical Analyzer. The sample used for thermal expansion measurements has been previously shown in Figure 4. The sample was positioned upright on a level quartz base, and a probe was lowered so that it just touched the surface of the sample. As the sample expands, the movement of the probe generates a signal, and a transducer converts the signal to a change in dimension. A 500 milligram weight was placed on top of the probe. The purpose of the weight was to insure good contact between the probe and the surface of the sample, as well as to aid in the determination of the glass transition temperature. A small, responsive oven encloses the sample. The operating conditions for all of the runs

was a controlled temperature ramp at 5 °C per minute from room temperature to 275 °C.

A typical thermal expansion diagram is shown in Figure 41, Appendix A. The y-axis denotes the change in dimension of the sample. The change in dimension is internally calculated by the instrument by dividing the current change in length of the sample by the original length of the sample. The x-axis denotes the temperature. The two curves shown in figure are the signal (top line) and the first derivative of the signal (bottom line). The thermal expansion coefficient is the slope of the signal line, and has the units of (length) / (length * temperature).

The TMA was also used to determine the glass transition temperature of the electromagnetically cured epoxy resin samples because glass transition measurements using DSC on the electromagnetically cured samples were inconclusive. When the glass transition temperature of the epoxy resin was reached, the glassy sample softened, and the weight placed on top of the probe contributed to the penetration of the probe into the sample. This is noted by the small hitch in the signal curve. The minimum of the first derivative curve is generally noted as the glass transition temperature.

Mechanical Testing

Samples were mechanically tested with the use of a uni-axial tensile testing instrument. The tensile testing instrument used in this study was the Instron TTC. The purpose of a tensile testing instrument is to measure the buildup of force or stress in the sample as it is being deformed. Important material properties that can be calculated from the result of tensile test were the Young's modulus and the tensile strength of the material. The sample used for mechanical testing has been previously shown in Figure 5. The sample is placed between two serrated grips and tightened, so that the slippage or release of the sample during testing is not possible. The sample is deformed by elongating it as it is held in place by the two grips. The load cell, which measures the buildup of force or stress, was calibrated in the range of 0 to 200 pounds by using free weights. The sample was elongated at the rate of .05 inches per minute. A typical stress-strain diagram is shown in Figure 42, Appendix A. The x-axis denotes the force or stress buildup in the sample, while the y-axis represents the strain undertaken by the sample.

PROCESSING

Thermal Processing

Thermal processing of the samples was performed in a Blue M forced air oven. A temperature controller kept the processing temperature to ± 1 °C of the set point temperature. For physical and mechanical property tests, four different isothermal cure cycles were used. The duration of each particular cycle is illustrated in Table 1.

Table 1 Thermal Processing Cycles

Temperature	Time (minutes)						
	30	60	90	120	180	240	360
140 °C			x	x	x	x	x
160 °C		x	x	x	x	x	x
180 °C		x	x	x	x	x	x
200 °C	x	x	x	x	x	x	

The rate of the epoxy-amine reaction is dependent on the temperature at which the material is cured. At lower temperatures (140 °C), it took a minimum of 90 minutes of curing time for the sample to strong enough to test. Longer times at higher curing temperatures (200 °C) were not considered because the reaction achieved completion.

Particular attention during thermal processing was addressed to insuring that there was uniformity of the cure throughout the entire sample. The extent of cure for each of the thermally cured samples were taken in three places: the center of the dog-bone and the two neck regions. The extent of cure at these three points were consistent with each other within the sample. From this, it was determined that the sample was uniformally cured. The extent of cure profiles for these processing cycles are shown in Figure 6.

Electromagnetic Processing

Epoxy resin samples for physical and mechanical properties were processed successfully in a singlemode electromagnetic cavity. Attempts to process physical and mechanical property testing samples in a multimode cavity were performed, however they were unsuccessful.

Singlemode Processing

Samples were placed in a seven inch diameter cylindical brass cavity. A representation of the microwave circuit is shown in Figure 7. Microwave energy at approximately 2.45 GHz was generated from an Opthos source. A coaxial cable was attached to the source and the energy was passed through a 20 dB directional coupler. The purpose

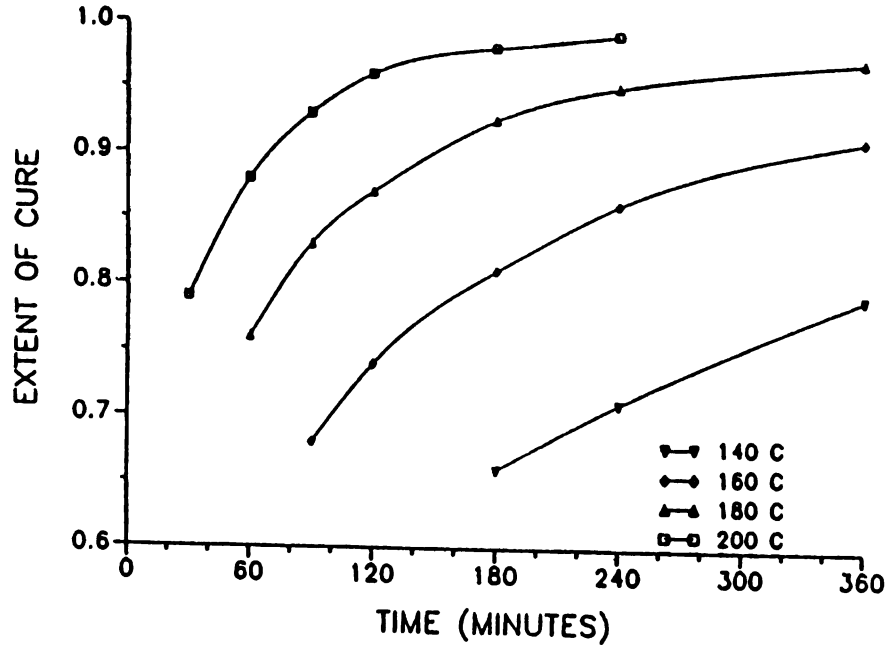

Figure 6). Extent of cure profiles for thermally processed samples.

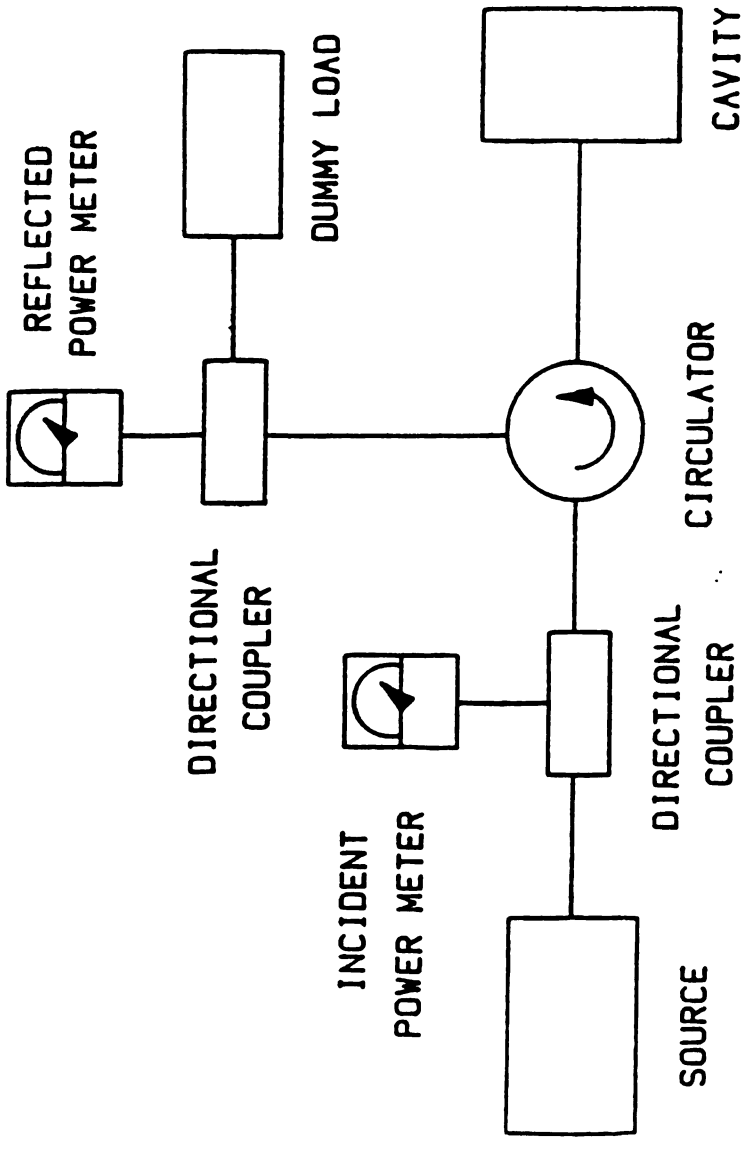

Figure 7). Representation of singlemode electromagnetic circuit.

of a directional coupler is to sample the power being passed through the circuit at that point. The sampled, incident power is led into a power meter. This incident power meter will give the measure of the approximate power passing through the circuit and the cavity. The non-sampled portion of power (87%) is directed towards a circulator. The purpose of a circulator is to prevent any relected power to return to the Opthos source. If reflected power returned to the source, the source would burn out.

The incident power passes through the circulator and is channeled into a coupling probe. The incident power enters the cavity through the coupling probe. For the singlemode case, the cavity and the sample absorbs 98+ percent of the incident power. The power that is not absorbed by the sample is called the reflected power. This power is guided into the coupling probe and proceeds backwards through the circuit to the circulator. The circulator directs the reflected power into another directional coupler. A sample of the reflected power is sent to another power meter. The unsampled portion of the reflected power is absorbed by a dummy load.

The difference between the incident power and the reflected power will be the power dissipated in the cavity and in the sample. The ratio of the absorbed power to the incident power will give a measure of the efficiency of the

system. The efficiency of this system is generally 98 percent or greater. This high efficiency can be attributed to the continuous adjustment of the cavity length and the coupling probe depth. The cavity length, along with the coupling probe, can be adjusted to minimize the reflected power during the course of a processing cycle.

The 7" diameter, cylindrical, cavity was operated in the TE_{111} mode. An experimental diagram of the power density contour lines of a 6" diameter diagnostic cavity when operated in the TE_{111} mode is shown in Figure 8 (31). A 6" diameter cavity develops the same power density contour lines as a 7" cavity. The heating pattern only has Φ and R direction components. The magnitude of the power density across the center line of the 6" cavity is shown in Figure 9 (31).

Since the field strength is position dependent, the location of the sample in the cavity is another important consideration when processing epoxy resins. The sample was placed in the cavity in the position shown in Figure 10. The sample was located 8 millimeters above the bottom by the use of a second silicon mold. The power density contour lines (Figure 9) in this location of the cavity where the sample was located are fairly uniform. This enabled a uniform, consistent, and reproducible heating of the particular sample.

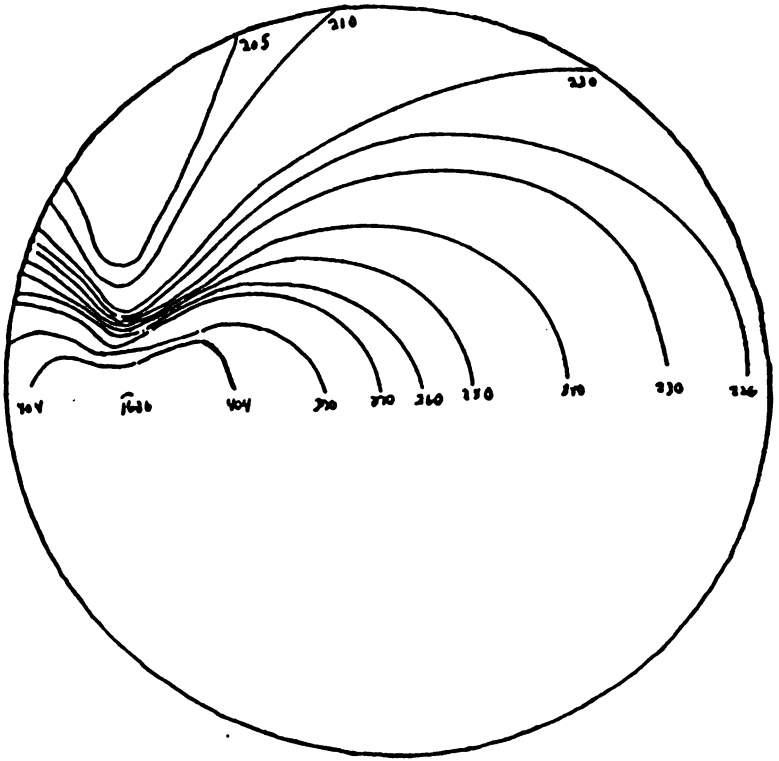

Figure 8). Diagram of power density contour lines in a 6 inch diameter cavity for TE_{111} mode.

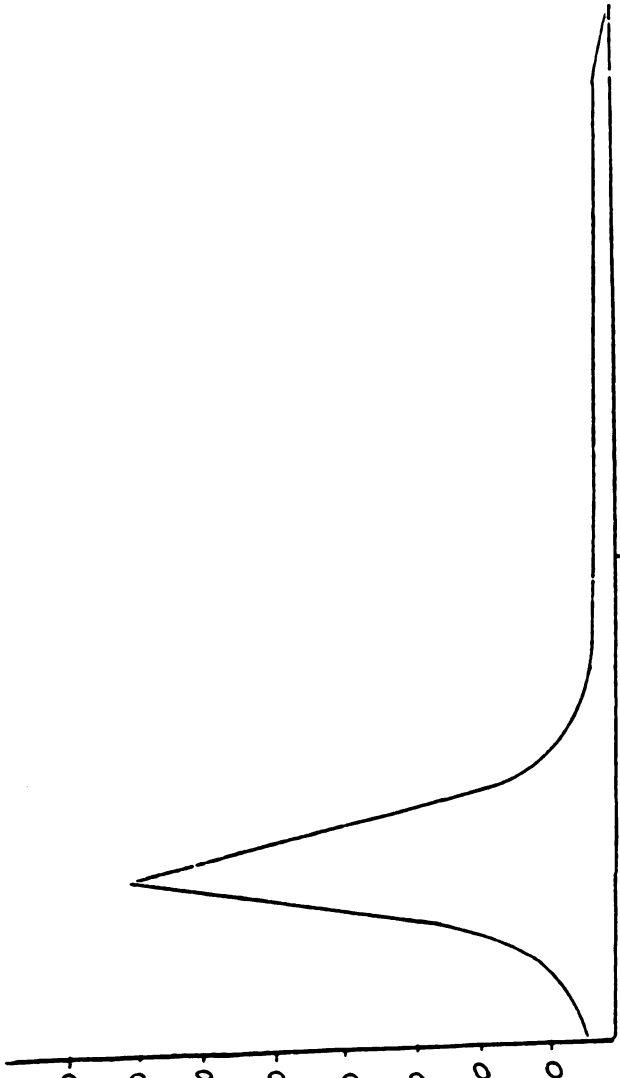

Figure 9). Diagram of the magnitude of the power density across the center line of a 6 inch cavity.

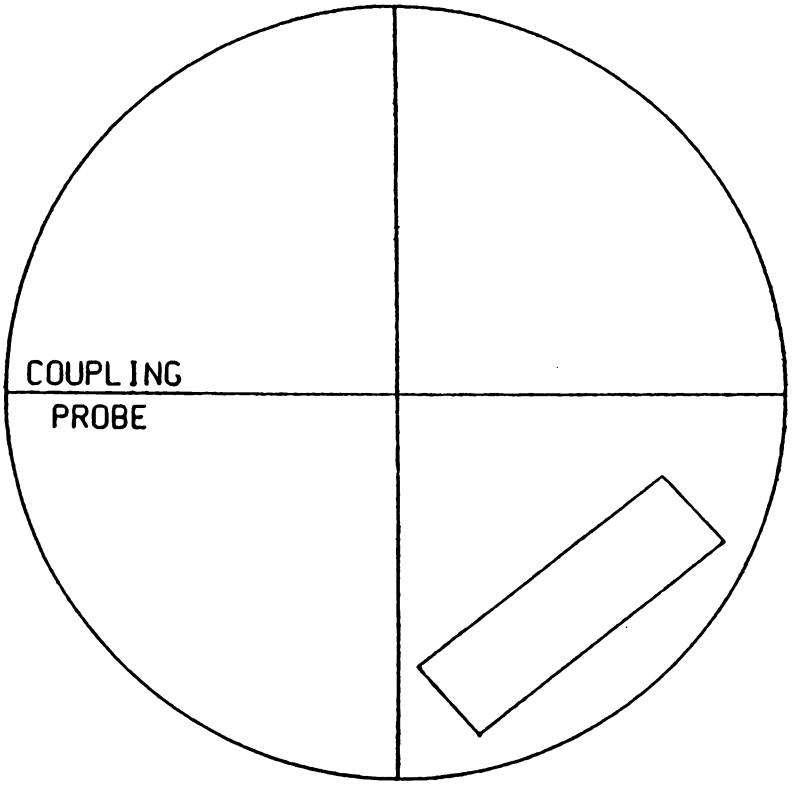

Figure 10). Diagram of the location used to process samples electromagnetically in a singlemode cavity.

The power density and field strength patterns are affected by the introduction of a sample in the cavity. These patterns will shift somewhat, and the shift is dependent on the location of the sample. Originally, samples were placed in the middle of the center line of the cavity. However, non-uniform heating in the sample occurred because the sample itself crossed many power density contour lines. Also, the left hand side of the dog-bone sample was close to the coupling probe, and this resulted in the boiling and burning of the resin in this area.

Two constant power cycles were experimentally determined to be applicable to the processing of epoxy resin dog-bone samples. A cycle that used too little power would never heat the resin up to the cure temperature. A cycle that used too much power would cause boiling and/or burning of the resin. The two cycles that were identified consisted of varying time intervals of 12.5 watts and 15.0 watts of incident power and are shown in Table 2.

Temperature profiles in the center of the dogbone sample for the electromagnetic cycles are shown in Figure 11. It is apparent that microwave energy can produce an instant temperature increase in a sample. The exothermic nature of the epoxy-amine reaction also contributes to the temperature increase. The exothermic peak seen is more pronounced as

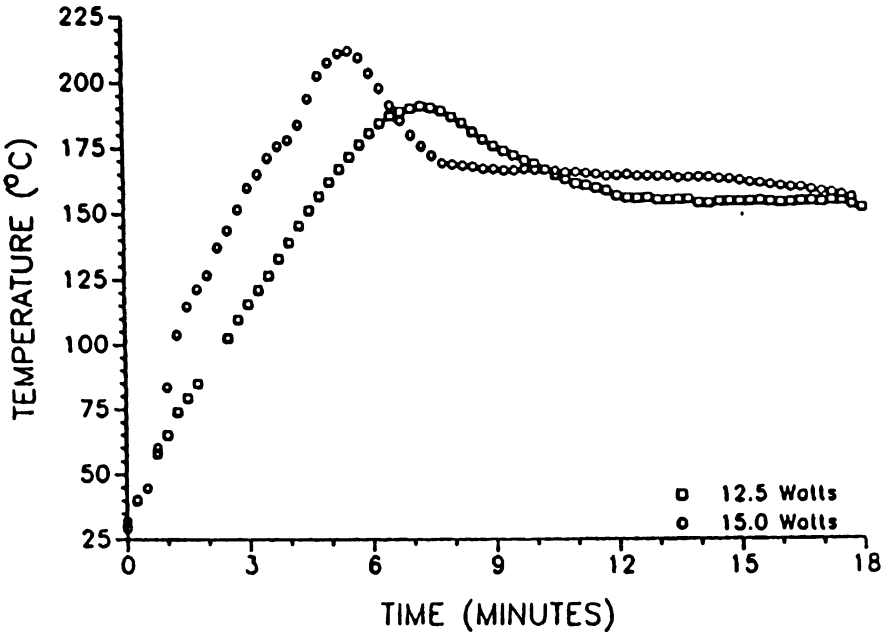

Figure 11). **Temperature profiles in samples during electromagnetic processing in a singlemode cavity.**

the power level is raised. When longer times are reached, the reaction subsides, and the sample eventually cools down to a steady-state temperature.

Table 2 Electromagnetic Processing Cycles

Power (Watts)	Time (Minutes)			
	30	45	60	90
12.5	x	x	x	x
15.0	x	x	x	x

The reflected power during the processing was less than one percent of the incident power. During the initial heating process, the reflected power was zero. As the sample heated up, the viscosity of the material decreased, and the mobility of the molecules increased. The enhanced mobility of the molecules increased the dielectric loss factor of the material. The increased dielectric loss factor increased the power absorption capability of the sample. As the sample cured, and the viscosity of the material increased, the dielectric loss factor decreased slightly due to the reduced mobility of the molecules to the electric field. This accounted for the slight increase in the reflected power during the later stages of the process.

A third cycle that combined electromagnetic with thermal

processing was also identified. The microwave component of this cycle was the initial curing of the samples for 15 minutes at 12.5 watts. The samples were approximately 60 percent cured after this first stage. The samples were then placed in a 180 °C thermal oven for additional curing of 15, 30, 45, and 75 minutes. Particular attention was paid in insuring that the electromagnetically cured samples were uniformally cured. Similar dissection analysis that was performed in the thermally cured samples was applied to the electromagnetically cured samples. This was especialy important in the electromagnetic case due to the non-uniformity of the power density contour lines found within the 7 inch diameter cavity. The extent of cure profiles for the electromagnetic and combination processed samples are shown in Figure 12.

All the samples that were electromagnetically cured in this study were performed in the TE_{111} mode. The samples that were cured were all placed on the bottom of the cavity. By adjusting the length of the cavity and the critical coupling probe distance, other modes and configurations are possible within the 7 inch diameter cavity. In some cases, samples would needed to be suspended above the bottom of the cavity in order to be cured when using these other modes.

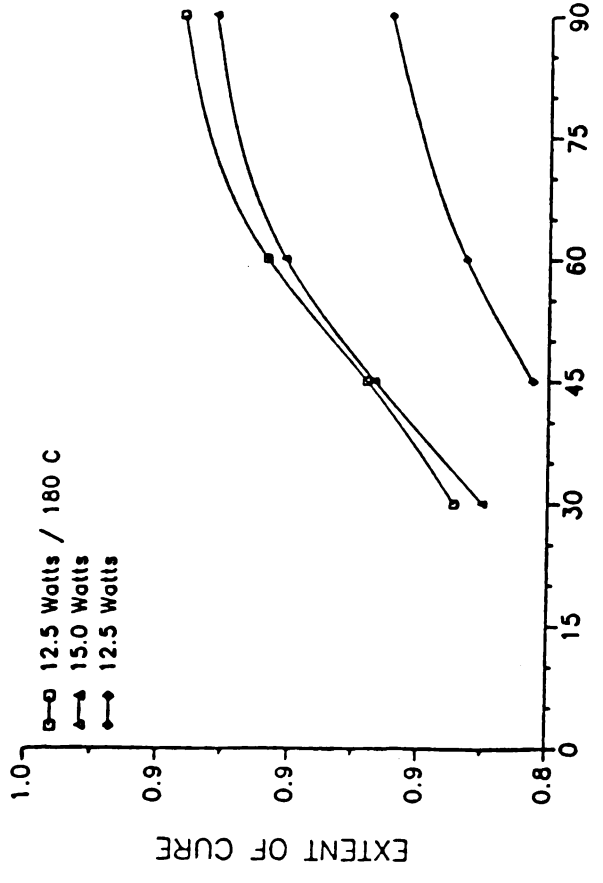

Figure 12). Extent of cure profiles for electromagnetic and combination processed samples.

Multimode Processing

The second technique that was used to process dog-bone samples electromagnetically was a multimode cavity. The dimensions of this cavity are 22 cm high, 33 cm wide, and 33 cm deep. A multimode cavity operates by having many modes simultaneously present in the cavity.

The first trial with this system used a Raytheon source which produced a maximum of 100 watts of power. The circuit diagram of the multimode setup is shown in Figure 13. This circuit is similar to the singlemode resonant cavity circuit in many respects. The dog-bone sample was placed on a teflon stand to elevate it off the bottom of the cavity. At the boundaries of the cavity, the field strength goes to zero. To help produce a uniform cure, a commercial microwave plate was used to rotate the sample. The plate rotated at a rate of one revolution every two minutes. Unlike the singlemode cavity, the multimode cavity can not be adjusted to minimize the reflected power. After 30 minutes in the cavity at 100 watts, a temperature increase in the sample was undetectable. Approximately seventy percent of the incident power was being reflected out of the cavity to the dummy load. Also, the rotating plate was absorbing some of the incident power. These two factors, coupled with the small size of the sample could explain why

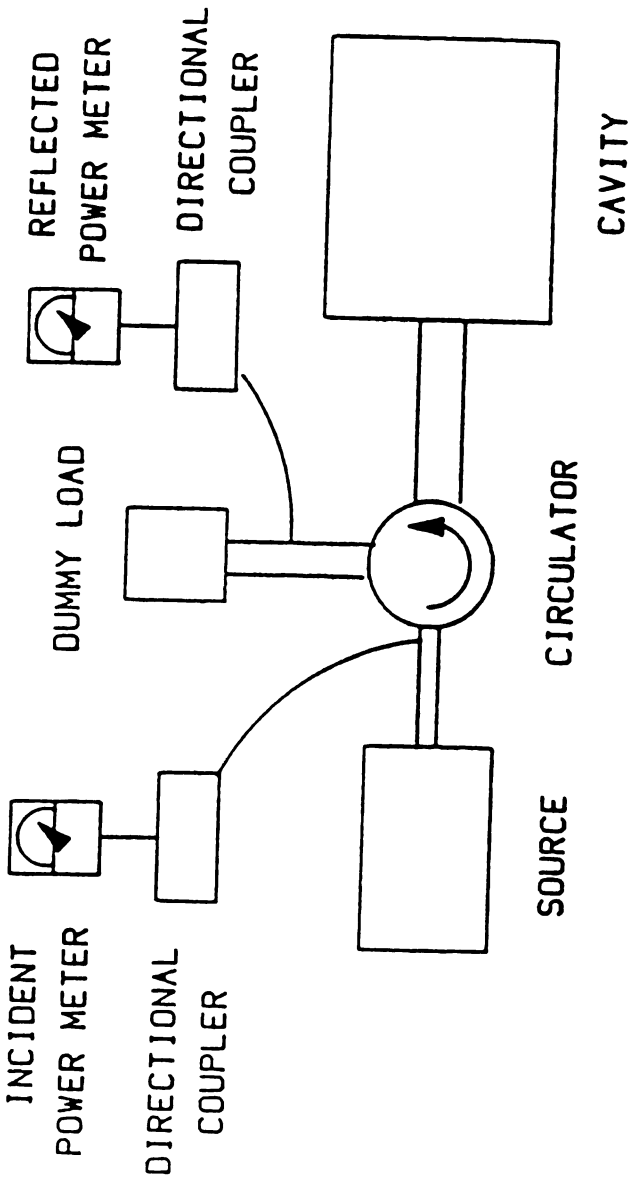

Figure 13). Representation of first multimode circuit used.

the sample never heated up.

A second attempt was made using a higher power Cheung source. The Cheung source could produce a maximum of 1000 watts of power. A representation of the circuit is shown in Figure 14. By increasing the power, it was thought that the dog-bone sample could absorb enough energy to heat up and cure. The sample was placed on the teflon ring, and the rotating plate was also used. Two hundred watts of power would produce a substantial temperature increase in the sample after five minutes in the multimode cavity. However, as the curing process proceeded, the temperature within the sample would decrease. Subsequent experiments utilized a varying cure cycle with several power levels being used. A cycle that was found to be adequate was a four step process. The first step was the initial heating and partial curing of the sample with an incident power of 200 watts for five minutes. The second step consisted of another 5 minutes of processing at 250 watts. The sample was approximately 50 percent cured at the end of the stage. The third stage was 5 minutes at 400 watts. Three possible power levels were identified to finish the curing of the sample. The power levels consisted of 500, 600, and 750 watts for varying lengths of time to produce the desired cure.

A problem existed because the rotating plate absorbed a significant amount of the incident power in the cavity.

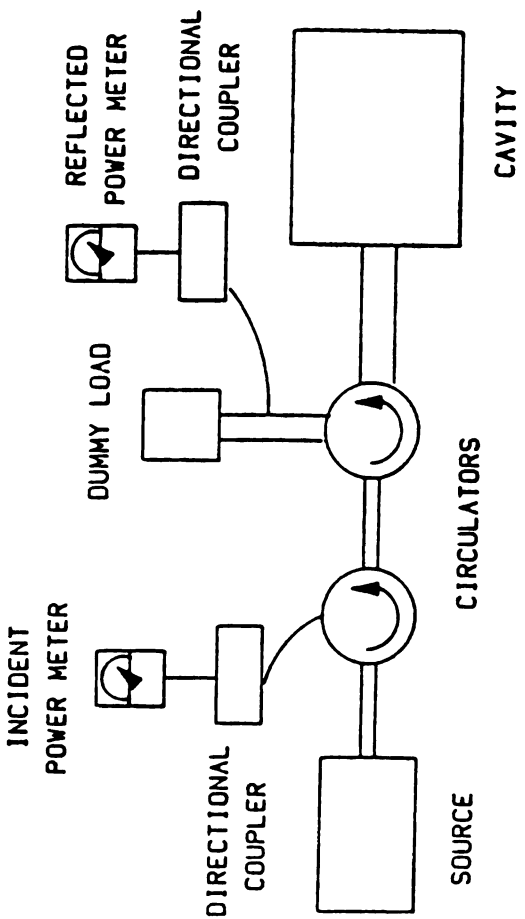

Figure 14). Representation of second multimode circuit used.

Eventually, after a considerable amount of time in the cavity operated at high power levels, the rotating plate melted. There was also a considerable amount of energy that was reflected back through the waveguide to the dummy load. The dummy load would absorb in excess of 500 watts of power, and water cooling had to be used to alleviate the possibility of heat-related damage to several components.

In order to process epoxy resins in a multimode system, the energy has to be coupled more efficiently into the sample. A carbon fiber, which is a conductor, was introduced into the dog-bone sample upon the belief that the energy would be absorbed along the fiber, and that would facilitate the curing process. A preliminary attempt using 25 watts of power to cure the sample was performed. A large portion of the power was absorbed along the fiber, and the fiber burned in the sample. This experiment, with careful control of the incident power level, could be used to successfully process a carbon fiber-epoxy resin sample.

RESULTS AND DISCUSSION

Certain physical and mechanical properties of the DER 332/ DDS epoxy resin system were studied. These properties were the glass transition temperature, thermal expansion coefficient, the Young's modulus, and the tensile strength. The Differential Scanning Calorimeter was used to determine the glass transition temperature, the Thermal Mechanical Analyzer was used to determine the glass transition temperature and the thermal expansion coefficient, and an Instron TTC were used to obtain the Young's modulus and the tensile strength of the material.

Glass Transition Temperature

The glass transition temperature of a sample gives an indication of the degree of cure and the amount of cross-linking present. The glass transition temperature is defined to be the temperature at which the material changes from a hard, brittle, state to a soft, rubbery state.

Two methods were used to determine the glass transition temperature. The glass transition temperature of the thermal and combination cured samples was determined by the Differential Scanning Calorimeter (DSC), while the glass transition temperature of the electromagnetic cured samples

was determined by the Thermal Mechanical Analyzer. Electromagnetically cured samples did not have a well defined glass transition temperature curve when determined by the DSC, and a thermal expansion method had to be used to accurately determine the glass transition temperature of the material. The second method to determine the glass transition temperature of a material was by the use of the Thermal Mechanical Analyzer (TMA). The thermal expansion method to determine the glass transition is discussed in the Experimental Procedures section. The glass transition temperature determined by the DSC is comparable to the glass transition temperature determined by the TMA.

The amount of cross-linking in the sample plays an important role in the glass transition temperature. As the amount of cross-linking increases, the glass transition temperature also increases. Samples that were thermally, electromagnetically and combination processed were all analyzed for a glass transition temperature. The glass transition temperature versus the extent of cure is shown in Figure 15. It is apparent from Figure 15 that the glass transition temperature is very sensitive to the extent of cure in the region where the extent of cure is very high.

The thermally cured samples had the highest glass transition temperature relative to the extent of cure when compared to the other two cases. A suggestion is that the

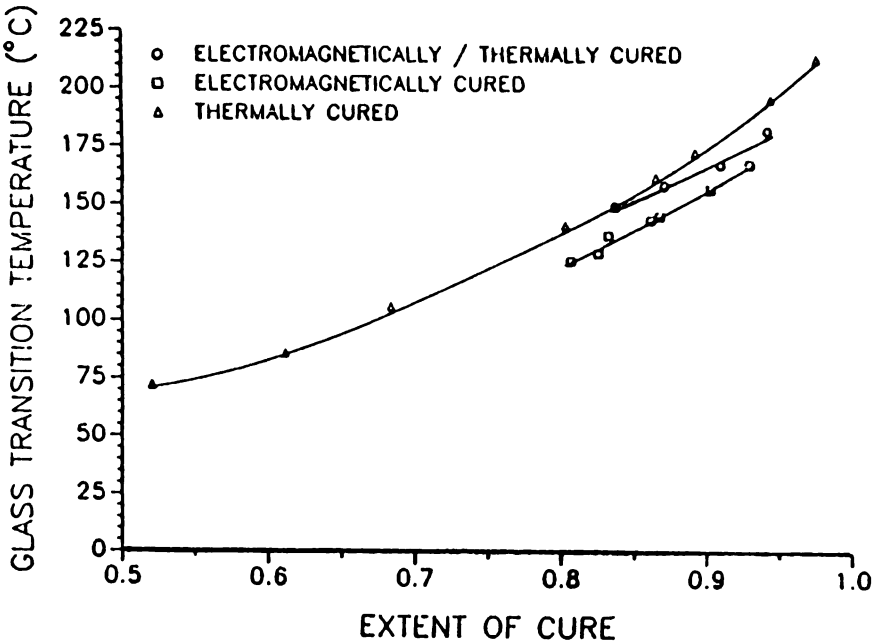

Figure 15). Glass transition temperature versus extent of cure for thermally, electromagnetically, and combination processed samples.

cross-link density in the electromagnetically processed samples is lower than the cross-link density of the thermally processed samples at the same extent of cure. The lower tensile strength found in the electromagnetically cured samples also suggests a lower cross-linking density.

The values for the DiBennedetto equation (3,4) for the three different processing cases along with literature data are shown in Table 3. The constant T_{go} is the glass transition temperature of the uncured material. E_x/E_m is the ratio of the lattice energies for cross-linked and uncross-linked polymers, while F_x/F_m is the ratio of segmental mobilities for the same two polymers. The data obtained from Bistrup, et al. (4) for the DER 332 / DDS epoxy resin system is also shown. Shown in Figure 16, is the curve for the calculated glass transition temperatures versus the extent of cure for Bidstrup's data, along with the thermally cured data obtained from this study.

Table 3 Values for the DiBennedetto equation for thermally, electromagnetically, and combination processed samples

Type of Processing	T_{go}	E_x/E_m	F_x/F_m
Thermal	9 °C	.65	.36
Thermal (4)	20 °C	.30	.18
Electromagnetic	18 °C	.56	.34
Combination	20 °C	.55	.33

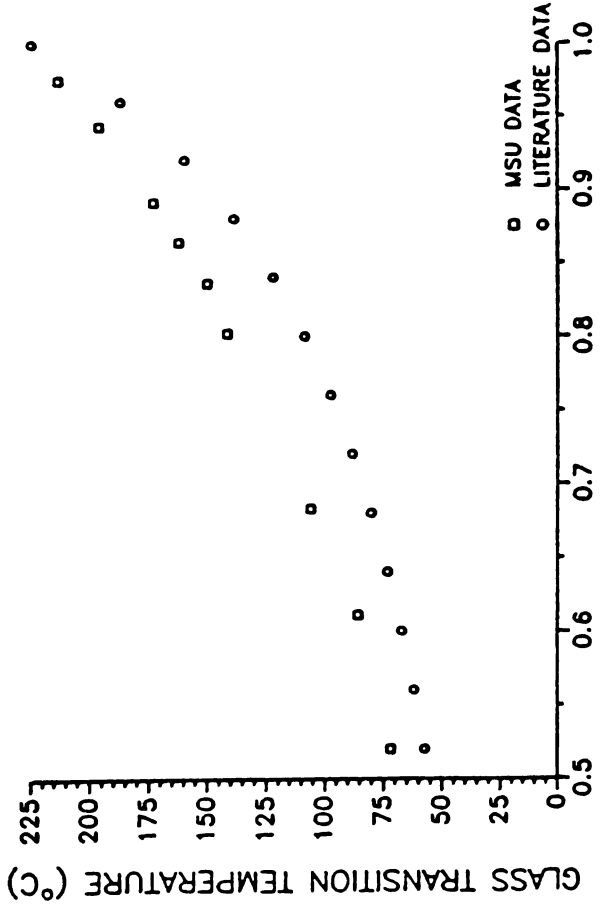

Figure 16). Glass transition temperature versus extent of cure for literature and present data.

The glass transition temperature of the DER 332/DDS epoxy resin has been determined by DSC after pulsed electromagnetic processing in the TM_{012} mode (11). The pulsed electromagnetic processing kept the samples under a constant temperature/time/position. The small, cylindrical, sample processed in the TM_{012} mode was oriented along the z-axis, suspended in the center of the cavity using a cotton string, and heated by the z-direction electric field of the TM_{012} mode. The sample holder was made of teflon. The glass transition temperature of these electromagnetically cured samples was also difficult to detect when using DSC. The results from this study show that the glass transition temperature of these pulsed electromagnetically processed samples is significantly increased when compared to thermally processed samples at the same extent of cure (11). However, the present work performed shows that there is a slight decrease in the glass transition temperature after electromagnetic processing of samples in the TE_{111} mode when compared to thermally cured samples at the same extent of cure. The samples shape used in this study has been described in Figure 5. The sample holder was made of silicon rubber and placed on the bottom of the cavity. The differences in the glass transition temperature between the two studies may be due to the nature of pulsed electromagnetic processing, the temperature/time history of the sample, and the effect of surrounding temperature using different materials as sample molds.

Thermal Expansion

Samples that were thermally, electromagnetically, and combination cured were tested. Samples that had an extent of cure of 80 percent or more were only tested. Samples that were less cured samples had a tendency to cure to the probe. The thermal expansion coefficient was calculated in 25 °C ranges from room temperature to where the glass transition temperature occurred.

Table 4 shows the thermal expansion coefficient, the standard deviation and the percent deviation for five temperature ranges from the 25 °C - 50 °C interval to the 125 °C - 150 °C interval. The extent of cure of the sample did not have an effect on thermal expansion coefficient. The thermal expansion coefficient was only a function of the temperature. The three different types of processing had identical thermal expansion coefficients within each temperature interval. Deviations ranged only two percent off of the averaged value. An overall thermal expansion coefficient was calculated by averaging the five intervals. The value for the 25 °C - 150 °C range was 62.9 μm/m°C. An overall thermal expansion coefficient was calculated through the software program for a single interval in the 25 °C - 150 °C range. This value was also 62.9 μm / m°C.

Table 4 The thermal expansion coefficient, the standard deviation, and the percent deviation for the five temperature intervals

Temperature Interval	Thermal Expansion Coefficient	Standard Deviation	Percent Deviation
25°C - 50°C	53.09 μm/m°C	0.9	1.7%
50°C - 75°C	62.68 μm/m°C	0.5	0.8%
75°C - 100°C	63.33 μm/m°C	0.4	0.7%
100°C - 125°C	65.33 μm/m°C	0.8	1.3%
125°C - 150°C	70.00 μm/m°C	1.6	2.3%

The thermal expansion coefficient above the glass transition temperature was also calculated. There was some dependence of the extent of cure on the values. The values for this thermal expansion coefficient are shown in Table 5. The increase in the thermal expansion coefficient above the glass transtition temperature suggests that the free volume of the sample increases steadily with increasing temperature.

Table 5 The thermal expansion coefficient versus the extent of cure above the glass transition temperature

Extent of Cure	Thermal Expansion Coefficient
0.80 - 0.85	120 - 140 μm/m°C
0.85 - 0.95	140 - 155 μm/m°C
≥ 0.95	155 μm/m°C

Young's Modulus

An important material property that can be calculated from the result of a tensile test is the Young's modulus. The Young's modulus is the measure of the resistance to the initial deformation in the sample as an external force is applied. The slope of the initial straight-line portion of the stress-strain diagram is used in calculating the Young's modulus of the material. A relationship which desribes the Young's modulus is:

$$E = \frac{(F / A)}{(\Delta l / L)}$$

where E = the Young's modulus
F = the external force applied
A = the cross sectional area of the sample
Δl = the change in length of the sample
L = the original or gage length of the sample

The Young's modulus have the same units as pressure (psi or GPa). The initial slope of the stress-strain curve can be represented by the quantity (F / Δl). Thus the modulus relationship can be reduced to:

$$E = \frac{SLOPE * L}{A}$$

The Young's modulus for the thermal, electromagnetic, and combination (electromagnetic and thermal) cured epoxy resin samples is plotted versus the extent of cure and is shown in Figure 17. The Young's modulus decreased linearly with an increase in the extent of cure for all three cases. The density and the intermolecular packing of the molecules are predominant factors in determining the room temperature modulus (22). The intermolecular packing of molecules in highly cross-linked systems is large because more free volume is trapped in samples with high glass transition temperatures. Because of this, one would expect a similar decrease in modulus when plotted against the glass transition temperature of the sample. A plot of the Young's modulus versus the glass transition temperature is shown in Figure 18. The figure indicates that the modulus decreases as a function of an increasing glass transition temperature. This tends to support the claim that systems which have more free volume trapped have a less brittle response. A plot of the modulus versus cure time is shown in Figure 19. As the

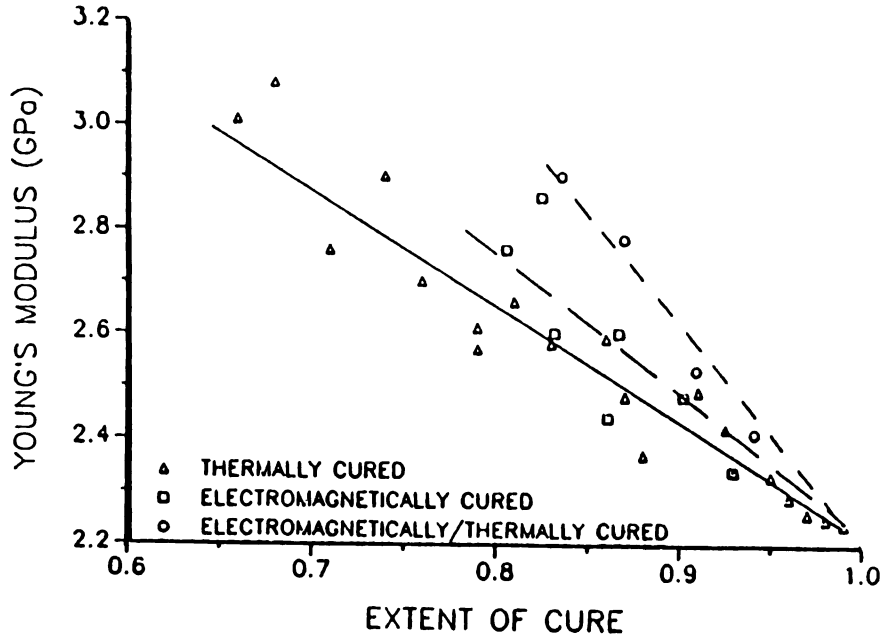

Figure 17). Young's modulus versus extent of cure for thermally, electromagnetically and combination processed samples.

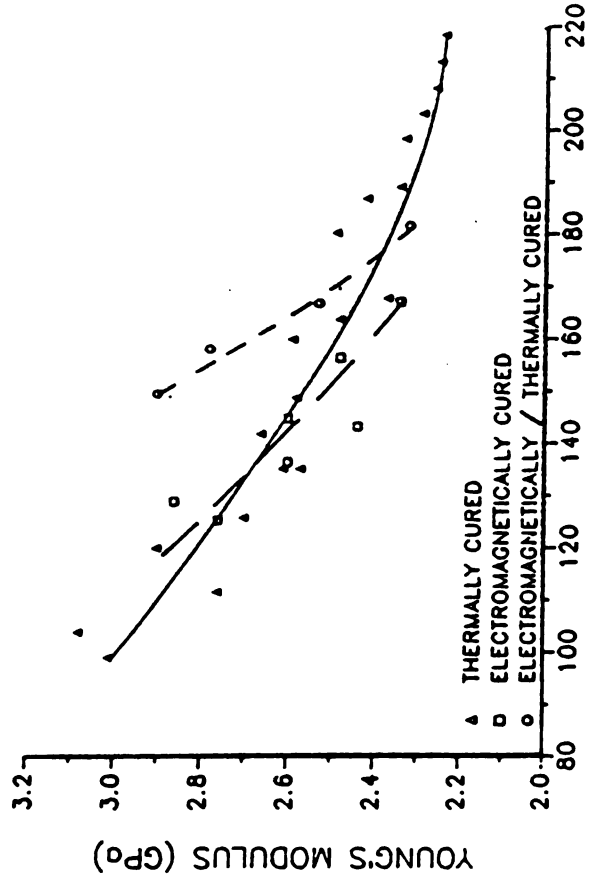

Figure 18). Young's modulus versus the glass transition temperature for thermally, electromagnetically, and combination processed samples.

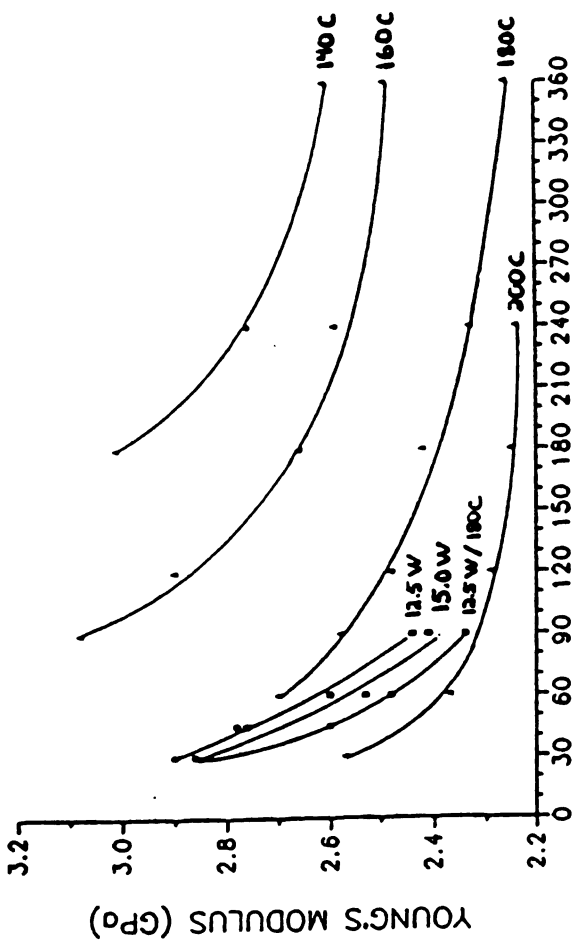

Figure 19). Young's modulus versus cure time for thermally, electromagnetically, and combination processed samples.

cure time increases, more cross-linking occurs, which results in a sample having more free volume and a lower modulus.

The samples that were electromagnetically or combination cured had a slightly higher modulus than the thermally cured samples with similar extents of cure. As the reaction approached completion, the values for all three cases were comparable. It would seem that the electromagnetically cured samples would have a lower free volume than thermally cured specimens, and this would result in a more brittle response, and ultimately in a slightly higher modulus. However, the free volume effect in electromagnetic processing has not been studied to date. An advantage of electromagnetic processing is that the time required to produce samples with a comparable Young's modulus was roughly 50 percent less in an electromagnetic applicator than in a conventional thermal oven.

Tensile Strength

Another important mechanical property that is calculated from a tensile test is the tensile strength of a material. The tensile strength is the maximum stress that the sample undergoes during a tensile test. A relationship which describes the tensile strength is:

$$TS = \frac{F}{A}$$

where TS = tensile strength
F = the maximum force applied to the sample
A = the cross-sectional area of the sample

The units of tensile strength are the same as the modulus. The tensile strength of DER 332 / DDS epoxy resin versus the extent of cure is shown in Figure 20. The tensile strength of the thermally cured samples had a slight increase until it reached a maximum of 95 MPa when the extent of cure was 80 percent. After reaching 80 percent cured, the tensile strength of the samples slightly decreased to a value of 75 MPa at complete cure. The phenomena where the tensile strength of a material is a maximum before complete cure is mentioned in (3). One would expect the tensile strength to increase with increasing cross-linking because Van der Waals bonds are being replaced with covalent bonds. It is presumed that microscopic cracks cause the reduction in tensile strength for a fully cured sample. The microscopic cracks develop from internal stresses caused by shrinkage or thermal changes in the molecular segments.

The tensile strength of electromagnetically cured samples increases dramatically as the extent of cure increases. As the reaction approaches completion, the

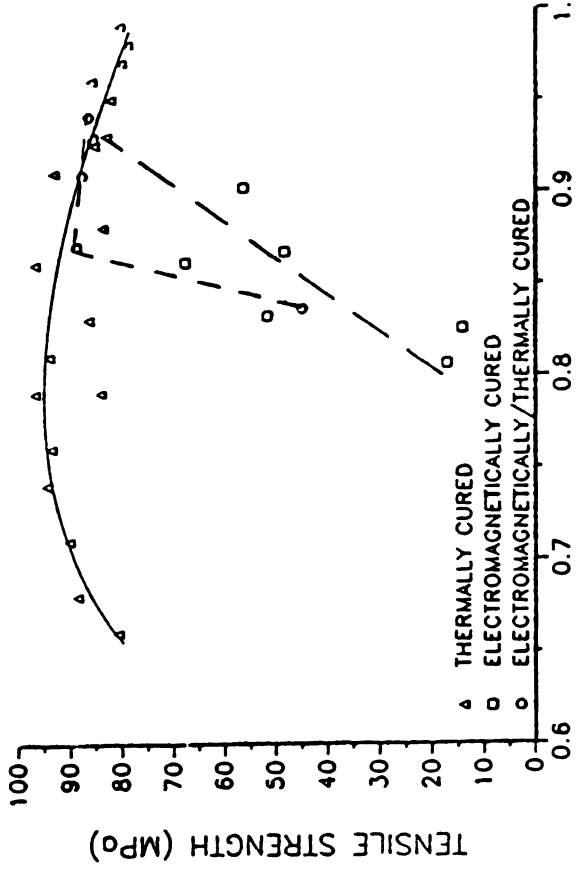

Figure 20). Tensile strength versus extent of cure for thermally, electromagnetically, and combination processed samples.

tensile strength for all three types of processing is comparable. The tensile strength of the samples that were electromagnetically processed was lower at similar extents of cure than thermally processed samples. The tensile strength of a sample is dependent on the cross-link density and the molecular arrangement within the sample. Therefore, the cross-link density and the molecular arrangement of the molecules in the electromagnetically processed samples is different than the thermally cured specimens with the same number of reacted groups.

The combination cured sample exhibits an interesting result. The first point, where the sample was cured 15 minutes at 12.5 Watts and 15 minutes at 180 °C, had an extent of cure equal to 84 percent, and a tensile strength midway between the thermal and electromagnetic processed curves. The sample was definitely affected by the initial curing by the electromagnetic energy. As the amount of thermal curing increases, the samples become less affected by the electromagnetic curing. As the thermal part of the curing cycle increased, the tensile strength values from the combination cured samples matched the values obtained from the thermally cured samples. An advantage of electromagnetic curing is that it produced samples with a comparable tensile strength in a reduced processing time as the reaction approached completion.

ONE-DIMENSIONAL MODELING OF THE CURE AND SIMULATION OF THE RESIDUAL STRESSES FOR THERMAL AND MICROWAVE CURING

Cure Simulation

Simulating the curing cycle of an epoxy resin system is of major importance. A computer simulation can give insight on temperature and degree of cure profiles, as well as optimizing the curing cycle to process the sample in the shortest amount of time possible. The temperature and degree of cure profiles are especially important in thick section materials where significant temperature gradients can lead to considerable degree of cure profiles in the material. The first step in developing a cure simulation is to determine the reaction mechanisms and kinetic expressions of the epoxy-amine system.

Reaction Mechanisms

Several possible reaction mechanisms exist for this epoxy-amine reaction. The first possible reaction is the reaction of the primary amine of DDS with the epoxy resin. The reaction chemistry for this case is shown in Figure 21. Another possible case is the reaction of the secondary amine with a another epoxide group. The chemistry of this case is shown in Figure 22. The products in both

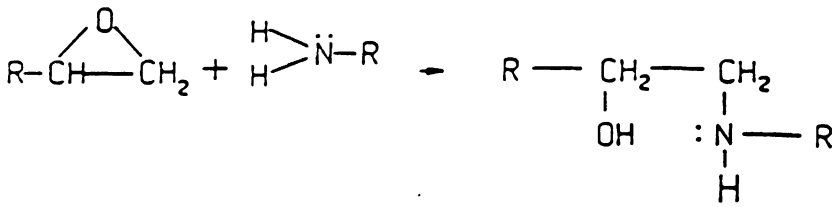

Figure 21). **Reacted structure from primary amine / epoxide group reaction.**

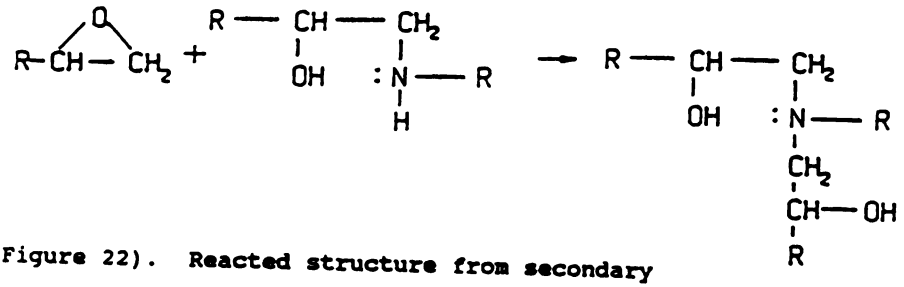

Figure 22). **Reacted structure from secondary amine / epoxide group reaction.**

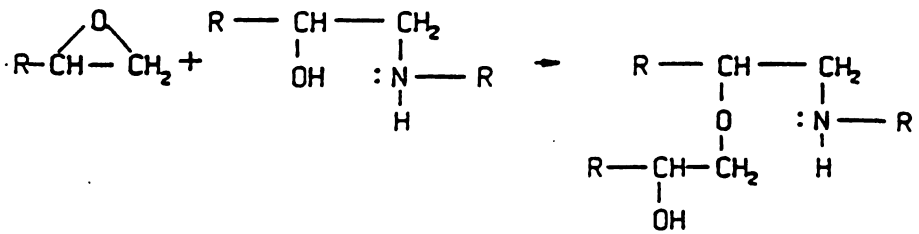

Figure 23). **Reacted structure from hydroxyl group / epoxide group reaction.**

these cases is a cross-linkage between the DDS molecule and the epoxy resin molecule. A hydroxyl group is also formed during these particular reactions. The hydroxyl functional group serves as the intermediate group in this autocatalyzed reaction. The hydroxyl group also plays an important part in the third reaction scenario (Figure 23). An ether cross-linkage is formed when the hydroxyl group reacts with an epoxide group in this case.

Reaction Kinetics

The epoxy-amine reaction in our particular study is considered to be an autocatalytic reaction. Autocatalyzed systems are characterized by the formation of some intermediate group, which accelerates the cross-linking reaction. In an autocatalytic reaction, the rate of reaction at the beginning is small because little product is present. The reaction rate increases as more product is formed, and then drops to a low level as the reactants become consumed. The maximum rate of reaction for an autocatalyzed system occurs when the extent of cure is approximately 30 - 40 percent.

From isothermal DSC runs, the kinetics of this particular epoxy-amine system can be determined. A basic assumption in DSC is that the heat flow is proportional to the reaction kinetics. The modeling of kinetics is

important because it can be used to optimize the processing conditions of the material. A DSC scan of an isothermal run at 220 °C is shown in Figure 43, Appendix A. First, the total heat flow is integrated to a point where there is no change in the heat flow (where the reaction stops). Second, a software program on the DuPont DSC was used to determine the number of joules per gram evolved from the sample at a particular time. Dividing these values by the total exotherm will give a profile of extent of cure versus time (Figure 24). Three separate isothermal curing temperature cases are presented in Figure 24. It is apparent to see how the curing temperature affects the reaction.

Temperature plays a very important part in the epoxy - amine reaction. From Figures 24 and 43, one can see that at an elevated temperature (temperatures greater than 200 °C) the reaction is approximately 75 percent completed before 15 minutes have elapsed. However, as the diffusion limitations of the reactants become important, it will take at least another 90 minutes to facilitate complete conversion of the reactants. If the epoxy resin is cured at a sufficiently low temperature (temperatures less than 170 °C), it is possible that the extent of cure will never reach 100 percent. The low temperature, coupled with high activation energies and diffusion limitation, will stop the reaction short of completion.

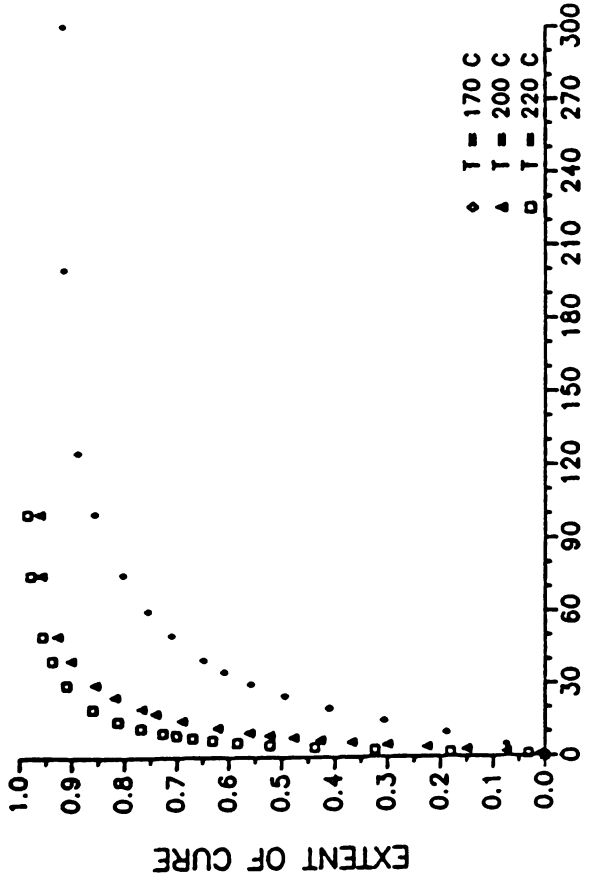

Figure 24). Experimental extent of cure versus time profiles for isothermal DSC runs.

Finzel (13), has reported the following equations which describe the DER 332 / DDS system with the 100 to 36 weight part fraction stoichiometry. The first equation, which is valid for systems which are less than 50 percent reacted is:

$$\frac{dx}{dt} = K1 * (1 - X)^2 + K2 * X * (1 - X)^2$$

where K1 = 1266650 * exp(-19400/RT)
K2 = 615.5 * exp(-11100/RT)

The second equation, which is valid for systems which are greater than 50 percent reacted is:

$$\frac{dx}{dt} = K3 * (1 - X)$$

where K3 = 5713.2 * exp(-1.9 * X) * exp(-13200/RT)

Two equations are needed to describe this system. The first rate equation represents the rate of reaction when the extent of cure is less than 50 percent. The second equation represents the rate of the reaction when the extent of cure is greater than 50 percent. Two different equations are needed to describe the system because the system changes from a free flowing reaction system to a diffusion limited reaction system when "gellation" occurs. Gellation is the point where the sample changes from a liquid to a solid. In this system, the gellation point occurs when the extent of cure is approximately 50 percent. When gellation occurs,

the reacting molecules have a difficult time trying to find one another due to the lack of mobility, and it results in a decreased reaction rate.

Thermal Simulation

A simulation incorporating the reaction kinetics and the physical properties of the DER 332 / DDS epoxy resin has been designed. The cure simulation uses a finite difference method to solve the non-linear differential equations over a time domain. A constant thermal diffusivity was assumed throughout the curing process. Both thermal and electromagnetic simulations were developed.

The cure simulation starts with a complete material and energy balance over the entire system. An equation which describes the material balance for the system is:

$$\frac{dX}{dt} = \frac{-r}{C_{ao}}$$

An equation which describes the rate of heat generated per unit volume from the chemical reaction is:

$$\frac{dH}{dt} = \frac{dX}{dt} * H_{rxn}$$

The differential equation that describes the heat

conduction and internal heat generation from the reaction in a one dimensional thermally cured sample is:

$$\rho * C_v * \frac{\delta T}{\delta t} = \kappa * \frac{\delta^2 T}{\delta x^2} + \frac{dH}{dt}$$

The left hand side of the equation is the energy accumulation term, while the first term on the right hand side is the amount of energy conducted into or out of the sample in the x-direction. The second term on the right hand side is the amount of energy generated from the reaction. A convective heat transfer boundary condition was also used.

$$h * A *(T - T_{air})|_{x=0,L} = \kappa * \frac{\delta T}{\delta x}|_{x=0,L}$$

The initial conditions used in the simulation are :

$$T = T_o \quad \text{for } 0 \le x \le L$$

The output from the simulation will give the temperature and extent of cure profiles in the sample during the curing process. Experimental temperature results from one centimeter thick samples which were thermally cured in a glass dish at 160 °C and 175 °C are shown in Figure 25 (13). Also shown in Figure 25 are the results from computer simulations which were run at the corresponding

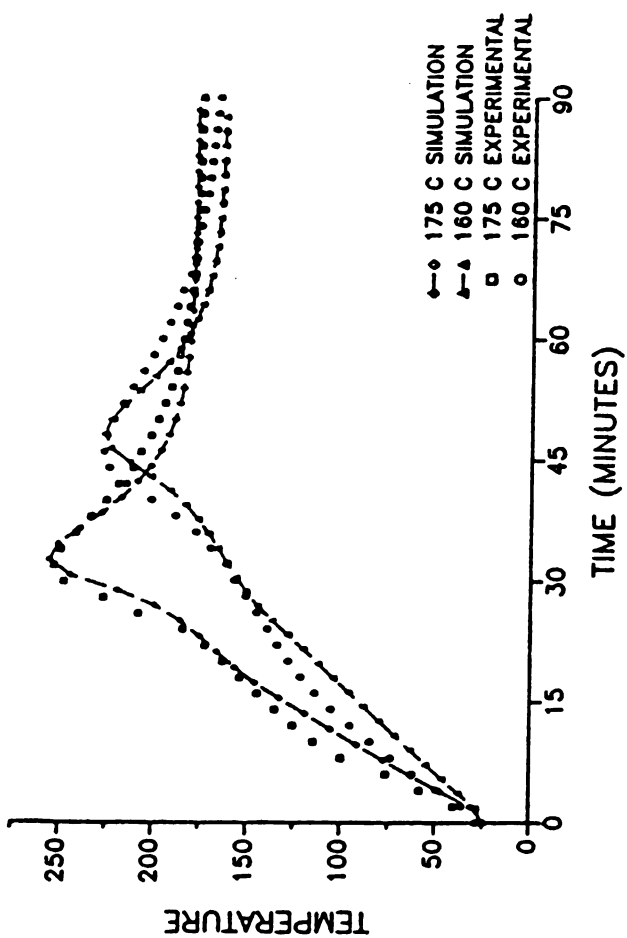

Figure 25). Experimental and simulated temperature results for a one centimeter thick sample thermally cured at 160 °C and 175 °C.

temperatures. The model does an excellent job simulating the temperature during the course of the reaction. The discrepency between the experimental and simulated temperatures at the beginning of the reaction can be attributed the the onset of convective flow in the resin.

The simulated center temperature profiles in one centimeter thick samples for 140 °C, 160 °C, 175 °C, and 200 °C curing temperatures are shown in Figure 26. As the curing temperature increases, the temperature difference between the center and the boundary increases. This difference reaches 100 °C when the curing temperature is 200 °C. The gradient develops because the reaction is exothermic, and the thermal conductivity of the material is low.

The simulated extent of cure profiles for the center of one centimeter thick samples for 140 °C, 160 °C, 175 °C, and 200 °C curing temperatures are shown in Figure 27. The elevated temperature found in the 200 °C cure temperature case accelerates the reaction. The 140 °C curing temperature case has a much slower reaction, and it will take a long time to achieve a complete cure.

The simulated center temperatures for 140 °C, 160 °C, 175 °C, and 200 °C curing temperatures versus the thickness of the sample are shown in Figure 28. The thickness of the

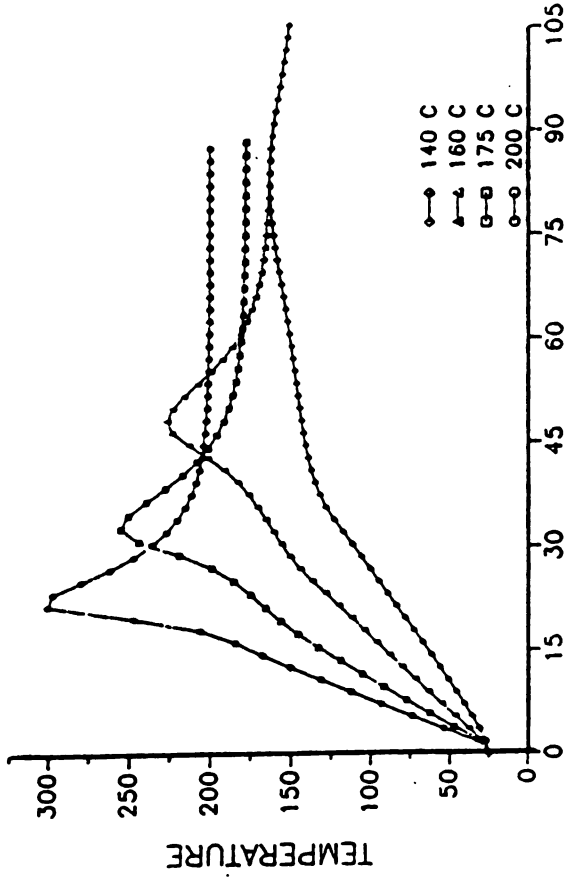

Figure 26). Simulated temperature profiles in the center of a one centimeter thick sample thermally cured at 140 °C, 160 °C, 175 °C, and 200 °C.

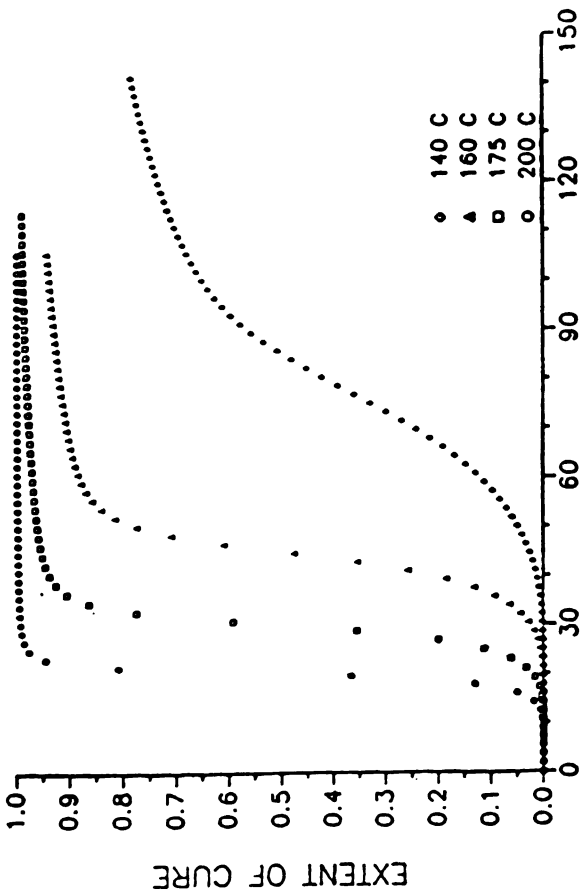

Figure 27). Simulated extent of cure profiles in the center of a one centimeter thick sample thermally cured at 140 °C, 160 °C, 175 °C, and 200 °C.

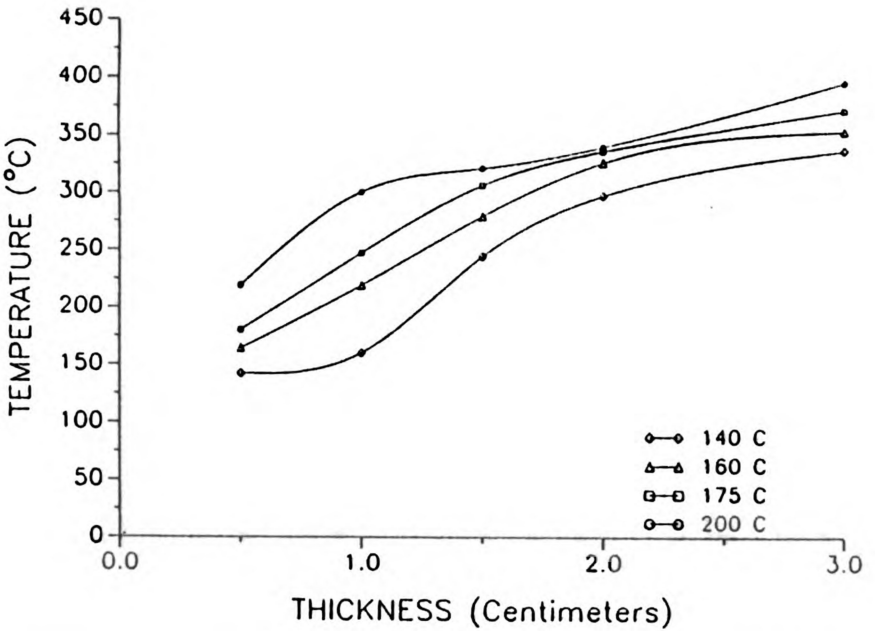

Figure 28). Simulated center temperatures in varying thickness samples thermally cured at 140 °C, 160 °C, 175 °C, and 200 °C.

samples range from 5 millimeters to 3 centimeters. As the curing temperature and the thickness increases, the maximum simulated temperature also increases. A thickness of 1.5 centimeters is required before the 140 °C cure temperature case develops temperatures much greater than the cure temperature. However, significant temperature departures from the cure temperature are found as early as 1 centimeter thick simulation in the 200 °C curing temperature case.

The simulated center temperatures profiles of varying thickness samples for a 160 °C cure temperature are shown in Figure 29. As the thickness of the material increases, the temperature gradient between the boundary and the center also increases. The center of a three centimeter thick sample reaches temperatures which are 200 °C higher than the curing temperature. The one centimeter thick sample has a center temperature of 75 °C higher than the curing temperature. The explanation for these large gradients is that as the curing temperature is reached, the reaction gives off heat as the reactants become consumed. Since the thermal conductivity of the material is low, the heat is converted directly into a temperature increase in the material. The temperature increase in the material increases the reaction rate. This circular cycle produces the extreme temperature gradients found especially in thick section samples. It is also apparent that the thicker the sample, the longer it takes to bring it to the reaction

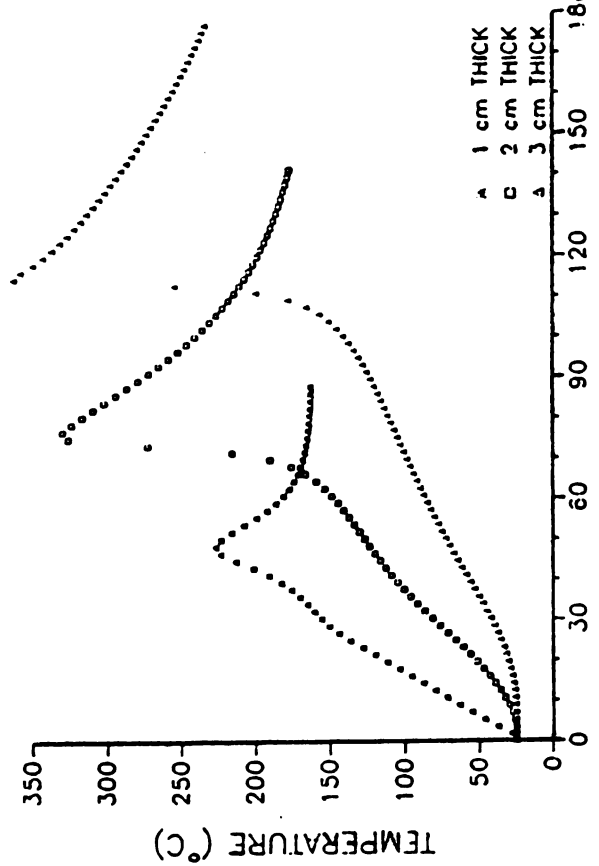

Figure 29). Simulated center temperature profiles in varying thickness samples thermally cured at 160 °C.

temperature.

The simulated temperature and extent of cure profiles within the samples for one, two, and three centimeter thick cases are shown in Figures 44-49, Appendix A. The simulation temperature used for all three thickness cases was 160 °C. This temperature allowed a one centimeter thick sample as well as a three centimeter thick sample to be cured. The one centimeter thick example (Figure 44) has three profile positions: Position 1 is at the boundary of the sample, at x = 0 cm.; Position 2 is midway between the boundary and the center of the sample, at x = 0.3 cm.; and Position 3 is at the center of the sample, at x = 0.5 cm. Sample symmetry is assumed throughout the simulation study, and other positions (0.5 cm. < x < 1.0 cm.) would only be repetitious.

From Figure 44, it is apparent that there really is not much of a temperature gradient as the material heats up. However, due to the exothermic reaction and the low thermal conductivity of the sample, the temperature in the internal section of the sample continues to increase, while the boundary temperature is controlled by the convective boundary conditions. A gradient of approximately 45 °C exists because of these factors. The temperature gradient manifests itself in a 10 - 12 percent extent of cure gradient in the sample. (Figure 45, Appendix A).

The simulated temperature and extent of cure profiles for a two centimeter thick sample cured at 160 °C are shown in Figures 46-47, Appendix A. The profile positions are: 1) the boundary, at x = 0 cm.; 2) the point midway between the boundary and the center, at x = 0.5 cm., and 3) the center of the sample, at x = 1 cm.. A small temperature gradient between the boundary and the center exists as the sample heats up. However, at the 60 minute mark, all three temperatures are identical. The two centimeter thick sample has a much sharper and larger temperature peak than the one centimeter thick sample. A gradient of 150 °C is evident in this example. The elevated temperature leads to a complete cure in the interior region of the sample. (Figure 47 Appendix A) The boundary of the sample exhibits appreciable cure earlier than the interior of the sample. However, the convection boundary condition limits the temperature found on the surface, and ultimately the extent of cure at the boundary.

Finally, the simulated temperature and extent of cure profiles for a three centimeter thick sample are shown in Figures 48-49, Appendix A. The profile positions for this example are: 1) the boundary, at x = 0 cm., 2) a distance one third of the way between the boundary and the center, at x = 0.5 cm., 3) a distance two thirds of the way between the boundary and the center, at x = 1 cm., and 4) the

center of the sample, at x = 1.5 cm. The surface of this sample heats up quite quickly when compared to the center of the three centimeter thick sample. As the entire sample reaches the cure temperature, the temperature of the interior section of the sample rapidly increases due to the previously discussed reasons. A temperature gradient of almost 200 °C exists between the boundary and the center during the peak of the reaction. This large temperature gradient is achieved in a relatively short amount of time (about five minutes). The three centimeter thick case is similar to the two centimeter thick case in many regards except that the temperature and extent of cure gradients are even more exaggerated.

Electromagnetic Simulation

A second preliminary, computer simulation has been designed for an electromagnetic simulation of the curing process of an epoxy resin. The electromagnetic simulation uses the same finite difference method found in the thermal simulation. A simple assumption in the electromagnetic simulation is that the power is absorbed equally throughout the sample at all times. This is an important assumption because the power absorption characteristics at a single location in the material is really a function of the temperature, dielectric loss factor and electric field

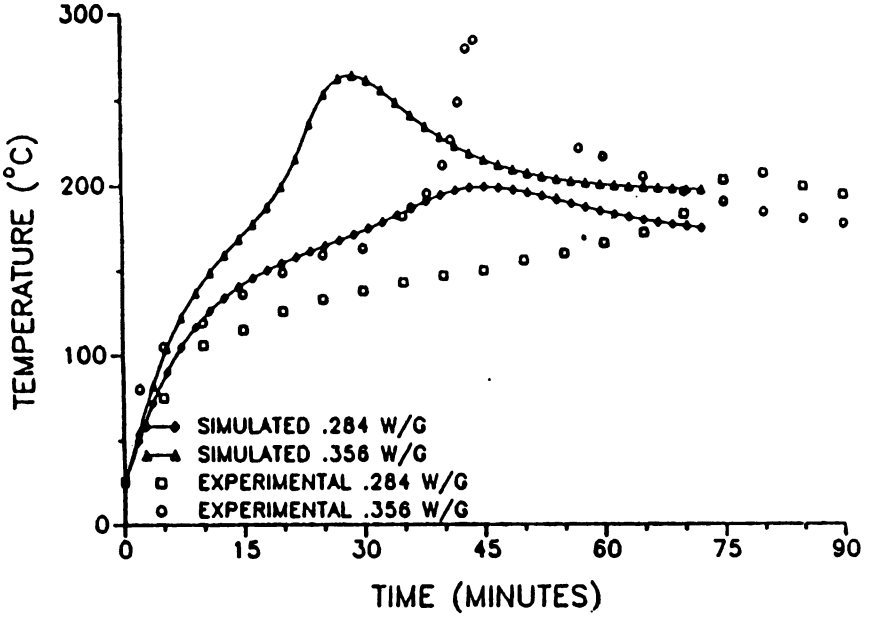

Figure 30). Experimental and simulated temperature results for a one centimeter thick sample electromagnetically cured at power densities of .284 watts per gram and .356 watts per gram.

strength at that particular location (11). Another assumption used is that the kinetic expressions for t electromagnetic system are the same as in the thermal system.

An equation which describes the electromagnetic curing process is:

$$\rho * C_v * \frac{\delta T}{\delta t} = \kappa * \frac{\delta^2 T}{\delta x^2} + \frac{dH}{dt} + \frac{P}{V}$$

where P/V = the power density of the electromagnetic energy directed into the sample

The equation is similar to the thermal simulation equation except for the addition of the electromagnetic energy absorption term. This term provides for an equal absorption of energy throughout the sample. Similar initial and convective boundary conditions used in the thermal simulation were applied to the electromagnetic simulation.

Experimental temperature results from multimode electromagnetic curing of a one centimeter thick epoxy resin sample in a glass dish are shown in Figure 30 (13). The two experiments had power densities of .284 watts per gram and .356 watts per gram respectively. The sample cured at the .356 watts per gram power density exhibited a larger and sharper exothermic temperature peak than the .284 watts per gram power density cured sample. The sample that was cured

at .356 watts per gram cured much faster than the .284 watts per gram sample. The computer simulations at the same power densities are also shown in Figure 30. Both simulations predict a quicker heating process and less intense exothermic peaks than their experimental counterparts. These effects can be the result of the equal power distribution assumption used. A cycle which uses a changing power density could be used to match the experimental to the simulated temperature profiles. It is apparent from Figure 30 that the sample is heating up too fast in the beginning which is a result of too much power. With a reduction in the initial power, the time it takes to reach the exothermic peak will also be longer. The simulations also predict larger exothermic peaks and shorter curing times when using higher power densities. These trends follow suit with the experimental results. The simulated extent of cure profiles for this example are shown in Figure 31. The higher power density sample cured much faster than the lower power density sample.

The effect of electromagnetic processing of different power densities on the thickness of samples has also been simulated. Figure 32 shows the center temperatures of varying thickness samples cured electromagnetically at power densities of .114 watts per gram, .150 watts per gram, and .175 watts per gram with a boundary temperature of 25 °C. As the power density and as the thickness increases, the

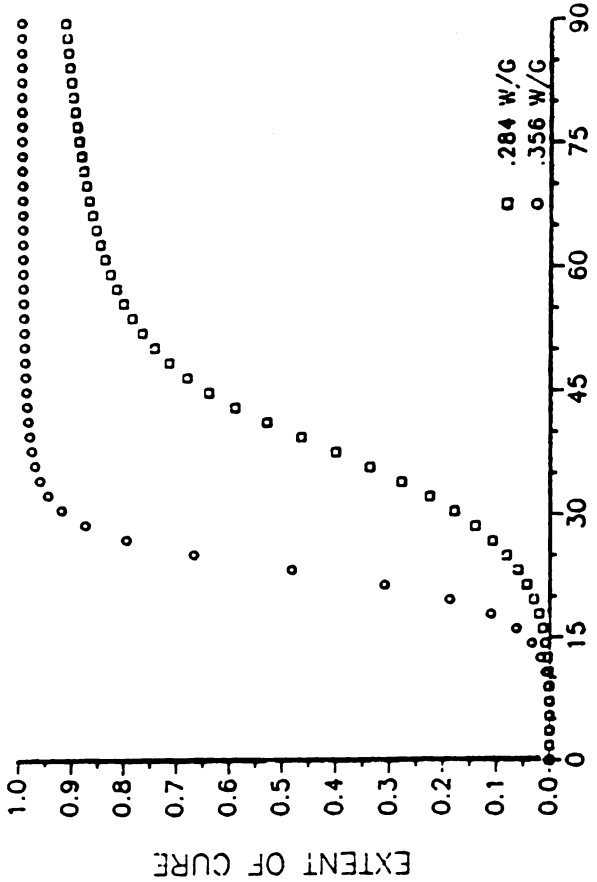

Figure 31). Simulated center extent of cure profiles for a one centimeter thick sample electromagnetically cured at power densities of .284 watts per gram and .356 watts per gram.

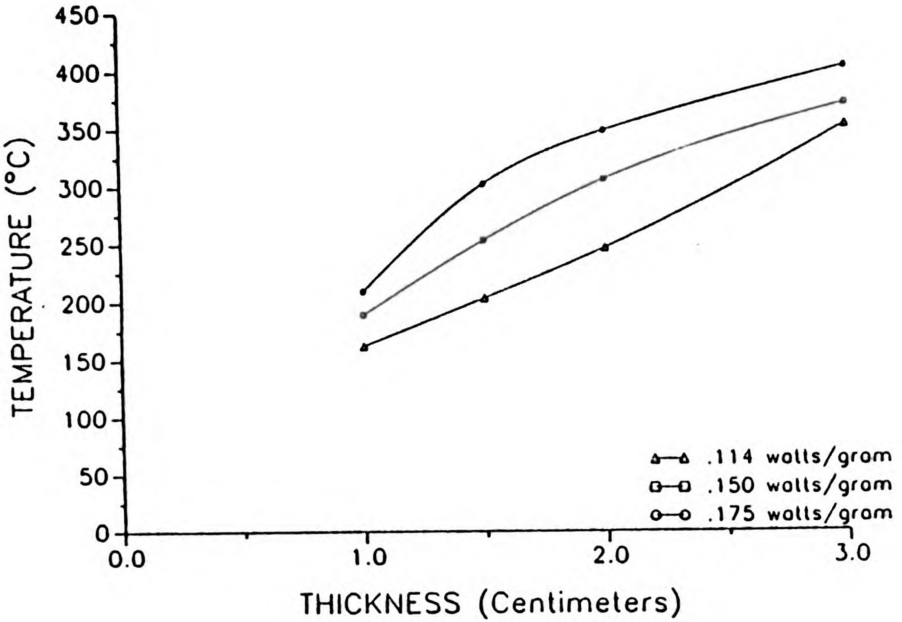

Figure 32). Simulated center temperatures for varying thickness samples electromagnetically cured at power densities of .114 watts per gram, .150 watts per gram, and .175 watts per gram with a boundary temperature of 25 °C.

center temperature also increases. Thin samples have reduced center temperatures than thick samples because the convection boundary condition is the limiting factor. A similar study with a boundary temperature of 100 °C has also been performed (Figure 33). Results are quite similar to the previous study except for a slight increase in the center temperature for all the cases. The slight temperature increase can be attributed to the reduction of the temperature gradient between the boundary and the center.

The effect of electromagnetic processing on the center temperature profiles of samples with varying thickness is shown in Figure 34. A power density of .114 watts per gram and a boundary temperature of 25 °C was used for each of these three examples. This power density was used because it could effectively cure a one centimeter thick sample, as well as a three centimeter thick sample. The initial heating period of the three samples (room temperature to 125 °C) are all identical. The similar power density being applied to each sample accounted for this phenomena.

As the temperatures in the material started to increase above the initial heating period, the convective boundary condition and sample geometry become more important. The three centimeter thick sample retained a greater portion of energy inputted into it, and exhibited a strong reaction

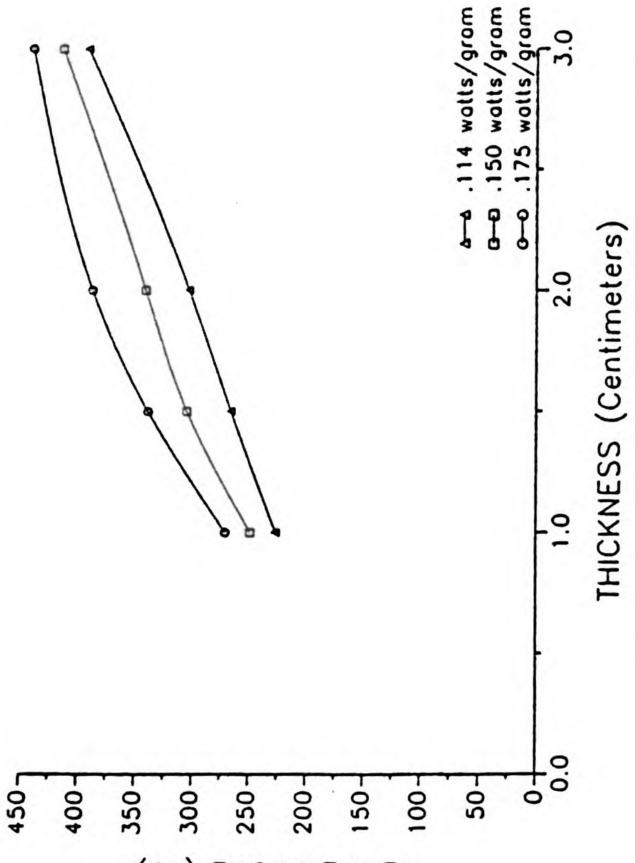

Figure 33). Simulated center temperatures for varying thickness samples electromagnetically cured at power densities of .114 watts per gram, .150 watts per gram, and .175 watts per gram with a boundary temperature of 100 °C.

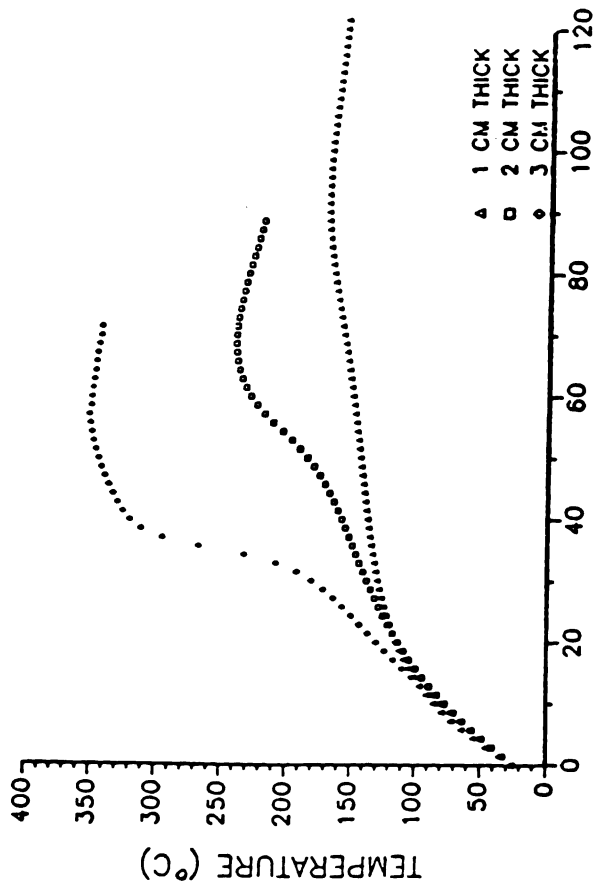

Figure 34). Simulated center temperature profiles for varying thickness samples electromagnetically cured at a .114 watt per gram power density.

exotherm at the 33 minute mark. The maximum temperature attained in three centimeter thick sample simulation is 353 °C. The two centimeter thick sample exhibited a slightly slower heating process, and a diminished reaction temperature peak. The one centimeter thick sample never really reached a temperature where a significant reaction can take place. The temperature during this simulation never exceeded 170 °C, and there is a small reaction exotherm at the 90 minute mark.

The temperature and extent of cure profiles for the one centimeter thick sample cured at a power density of .114 watts per gram are shown in Figures 50-51, Appendix A. The sample positions used in this study are identical to the sample positions used in the one centimeter thick thermal study. A temperature gradient of 20 ° C exists between the boundary and the center of the sample throughout most of the process. The temperature gradient causes a rather large extent of cure gradient in the sample. (Figure 51, Appendix A)

The results of a two centimeter thick sample simulation at a power density of .114 watts per gram are shown in Figures 52-53, Appendix A. The sample positions used in this example are the same as in the two centimeter thick thermal simulation. A temperature gradient of almost 50 °C develops in the sample. As in all electromagnetic simulations, the

30 °C air temperature convection boundary condition helped to contribute to the gradient. A large extent of cure gradient is also present in the sample. (Figure 53, Appendix A)

The temperature and extent of cure profiles for the three centimeter thick simulation cured electromagnetically at .114 watts per gram are shown in Figures 54-55, Appendix A. The profile positions used in this study are the same used in the three centimeter thick thermal simulation. Temperature gradients existed through much of this simulation. The maximum gradient was approximately 135 °C at the 70 minute mark of the process. From the extent of cure profiles, it is apparent that the entire sample is fully cured at the 70 minute mark.

The elevated temperatures found in the center of thick section simulations as well as in the center of thin sections simulated at a high temperature curing cycle contribute to the quick and complete reaction of the epoxy resin. These elevated temperatures can have a detrimental effect on the resultant properties of these resins. During extent of cure determinations in a DuPont DSC, temperatures above 330 °C caused decomposition of a sample. In many of these simulation studies (especially in thick section cases), temperatures easily exceeded the 330 °C decomposition point. When a material reaches its

decomposition point, the structural integrity of the material is of question.

Comparisons

There are some major differences between thermal and electromagnetic processing of epoxy resin samples. Thermal processing begins with the conduction and convection of energy into the sample from the boundary, while electromagnetic processing directly couples energy into the entire sample simultaneously. The amount of energy lost at the material boundary condition is more apparent in the electromagnetic simulations because T_{air} is only 30°C, while in thermal processing T_{air} is 140°C, 160°C, 175°C, or 200°C.

Higher curing temperatures and higher power densities result in sharper and larger temperature peaks caused by the exothermic reaction. Thicker samples had much larger temperature gradients between the boundary and the center than thinner samples for both types of processing. In a thermal environment, thick samples take longer to cure than thin samples. However, in an electromagnetic environment, thick samples can be cured in a shorter amount of time than thin samples.

RESIDUAL STRESS SIMULATION

Residual stresses in thermoset materials are caused by non-uniform cooling of a non-uniformally cured sample. These stresses have serious influences on the resultant mechanical properties of the sample. The non-uniformally cured material results from the temperature gradients apparent in the material during curing. The temperature gradients are caused by the highly exothermic reaction coupled with the low thermal conductivity in the sample. Larger temperature gradients are found in thicker samples, in samples processed at higher curing temperatures in a thermal environment, as well as samples processed at higher power densities in a microwave environment. The non-uniform cooling arises from the cooldown of the non-uniform material to ambient temperature from an elevated temperature.

Mechanism for Generating Residual Stresses

There are three steps which describe the mechanism for generating residual stress in samples. The first step is the cooldown of the sample from an elevated temperature to the glass transition temperature (T_g) of the material. At this point, there are no stresses in the sample. Stresses begin to originate when the temperature of the material is cooled below the glass transition temperature of the material. An explanation for this is that the network

segments become rigid, and relaxation of the segments is not possible. When the temperature of the material is above the glass transition temperature, relaxation of the network segments is possible and stresses cannot originate.

The second step is where the surface of the sample is quenched to ambient temperature (T_{amb}). The shrinkage on the surface is noted by the product of the thermal expansion coefficient (α) multiplied by the temperature difference ($T_g - T_{amb}$). The internal region of the sample still remains at the glass transition temperature, and stresses do not originate in the center of the sample.

The third step is the gradual cooldown of the entire sample to the ambient temperature. The internal region undergoes a shrinkage $\alpha * (T_g - T_{amb})$. The contraction of the hot, internal portion of the sample will cause tensile stresses in this region because the cool, external layer of the sample has been fixed. Thus, the external layer enters a compressive state and the internal region enters into a tensile state.

Stress Simulation

A finite element program was used to calculate the the residual stresses in a simulated sample. The program, CONCEPT™, is developed from a series of finite element

programs written by the Concept Analysis Corporation, Plymouth, Michigan. The finite element program was able to calculate the displacements and stress contour lines in a one-dimensional thick section epoxy resin sample. The fundamental equations which develop the finite element approach to solving residual stress problems are shown in Appendix B.

The origination of residual stresses in a sample is an unsteady state process due to the non-uniform cooling. However, the finite element program used was a steady state linear elastic analysis. The differential equations which describe the formation of residual stress due to an unsteady state process are shown below. The first equation can be used to evaluate the strain generated from the cooling process.

$$\int \int Er(t-\tau,T) \frac{\delta}{\delta\tau} \left\{ \epsilon(\tau) - \int \alpha(T)\delta T \right\} \delta\tau \, \delta x = 0$$

where Er = relaxtion modulus
t = time
τ = increment of time
T = temperature
ϵ = strain which is generated
α = thermal expansion coefficient

The second equation can be used to solve for the thermal stress directly from the displacements calculated from the previous equation.

$$\sigma_t(x,t) = \int Er(t-\tau,T) \frac{\delta}{\delta\tau} \left\{ \epsilon(x,\tau) \right\} \delta\tau$$

where σ_t = thermal stress

To model the stresses more effectively using the finite element program, the stress simulation was performed in two steps. The first step simulated the quenching of the surface of the sample from a glass transition temperature to the ambient temperature. The displacements generated from the first step were added to the boundary condition file used for the second step. The second step was the cooldown of the entire system to the ambient temperature. The three main data input sections for the program are the grid file, the element file, and the boundary condition file.

The grid file contains the geometry information of the system, and the element file contains the physical and mechanical property information of the resin, as well as the temperature information at the nodes. The extent of cure values, which are a part from the output from the cure simulation, were used in combination with the values experimentally determined for the DiBennedetto equation to determine the glass transition temperature at each of the nodes. A different set of material properties was used in each element because the non-uniform curing of the samples resulted in a sample with non-uniform properties. Each element also had a corresponding thickness of 1 millimeter. Since symmetry is being assumed throughout the study, the one centimeter thick samples used 5 elements, and the three centimeter thick samples used a total of 15 elements.

Simulations to determine the one-dimensional residual stress in thick section epoxy resins were performed. The effect of thickness and cure temperature on the residual stress profiles were studied for samples simulated in a thermal environment, and the effect of thickness and power density levels were studied on the residual stress profiles for samples simulated in an electromagnetic environment. The output from the residual stress simulation was the profile of the stress generated versus the depth in a material.

The simulated residual stress was plotted as a function of depth in the sample. Figure 35 shows the stress profile in a one centimeter thick sample thermally cured at 140 °C, 160 °C, 175 °C, and 200 °C. As the curing temperature increases, the stresses within the sample also increase. The maximum compressive stress encountered was 1.18 MPa at a curing temperature of 200 °C. The maximum tensile stress encountered was .70 MPa also at the 200 °C curing temperature. Samples cured at higher temperatures have higher glass transition temperatures than samples cured at lower temperatures. The higher glass transition temperature will ultimately increase the amount of shrinkage in the sample.

The effect of thickness on the residual stress profiles

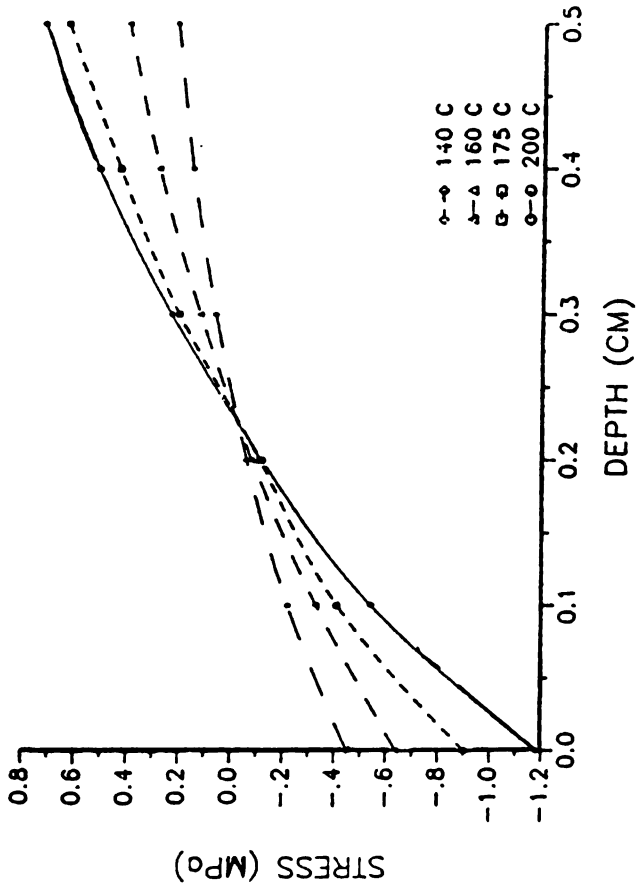

Figure 35). Residual stress profiles for a one centimeter thick samples thermally cured at 140 °C, 160°C, 175°C, and 200°C.

for thermally cured samples was also studied. One, two and three centimeter thick thermally cured samples at 160 °C were studied (Figure 36). Larger stresses resulted in the thicker samples. Due to the exothermic nature of the reaction, the thick samples had elevated temperatures which attributed to complete conversion of reactants to products in virtually the entire sample. The complete conversion of the reactants results in a material with a higher glass transition temperature. This will result in a sample with larger residual stresses.

The residual stress profiles for one centimeter thick samples electromagnetically cured are shown in Figure 37. The power densities used in the simulation were .284 watts per gram and .356 watts per gram. The higher power density resulted in a higher tensile and compressive stress. Three different thicknesses were also studied. These thicknesses were one, two, and three centimeters. The power density used for these simulations was .114 watts per gram. Like the previous thermal thickness study, the residual stresses increased in the thicker samples (Figure 38). The one centimeter thick sample had a very low stress level because the amount of curing was small. The three centimeter thick samples achieved almost a complete cure and develop larger magnitude stresses.

The values for the residual stress in the thick

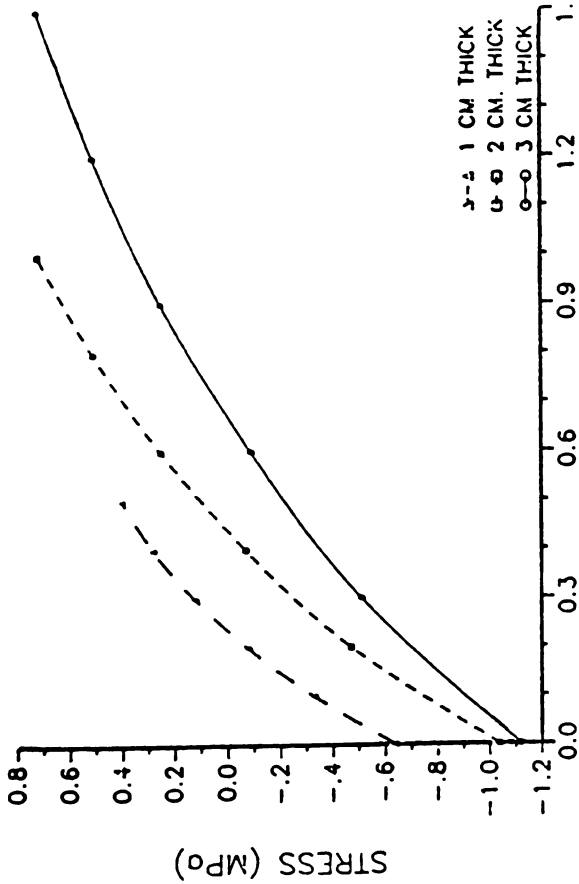

Figure 36). Residual stress profiles for one, two, and three centimeter thick samples thermally cured at 160 °C.

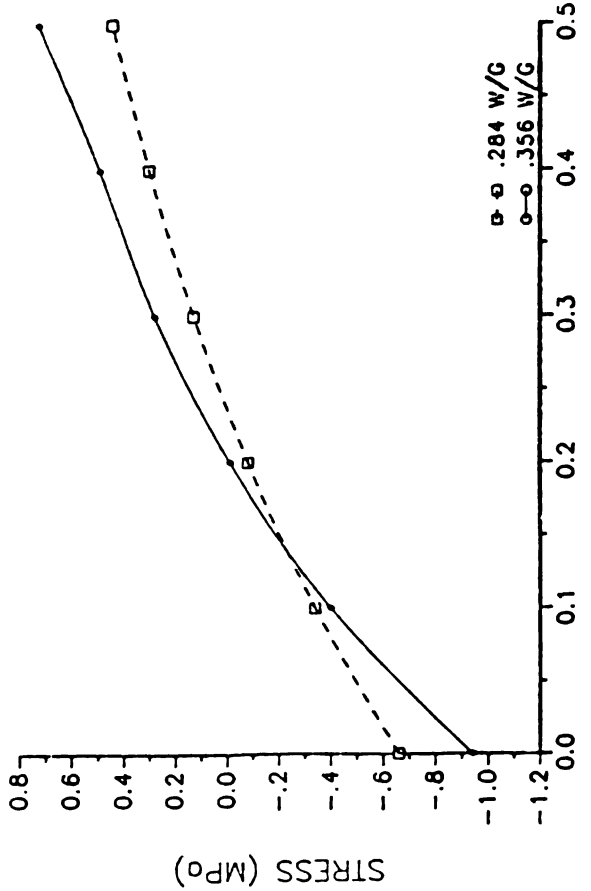

Figure 37). Residual stress profiles for a one centimeter thick sample electromagnetically cured at power densities of .284 watts per gram and .356 watts per gram.

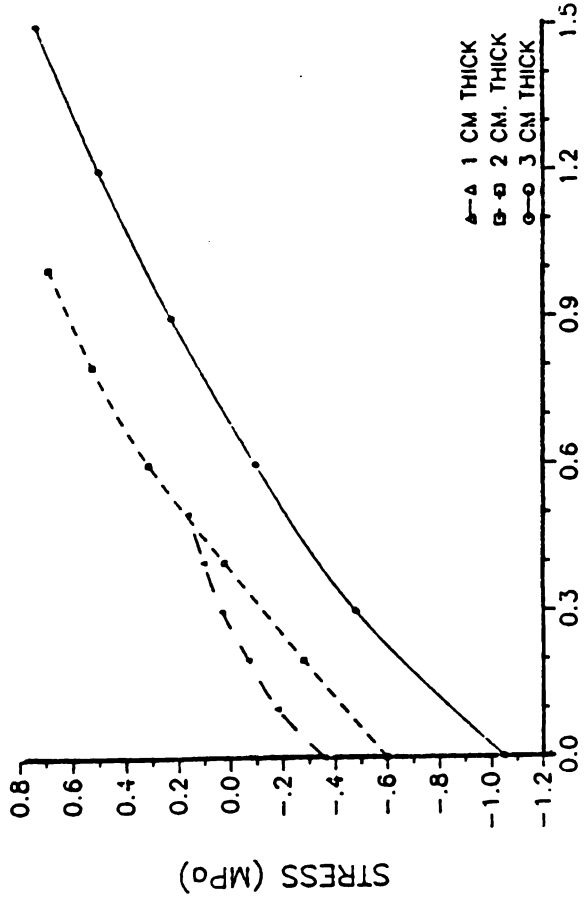

Figure 38). Residual stress profiles for one, two, and three centimeter thick sample electromagnetically cured at a power density of .114 watts per gram.

section, the increased temperature, or the increased power density case approached asymptotic values. As the extent of cure of a simulated sample for these cases approaches 100 percent, the glass transition temperature of the sample approaches its maximum. The temperature difference between the glass transition temperature and the ambient temperature becomes a maximum as the extent of cure approaches 100 percent. These asymptotic residual stress values were primarily determined by the amount of shrinkage accrued due to the cooling down of the material from a glass transition temperature to an ambient temperature $\alpha * (T_g - T_{air})$. These stress values were 1.2 MPa for the compressive stress in the external region of the sample, and .75 MPa for the tensile stress in the internal region of the sample.

Experimental Methods for Determining Residual Stresses

There are three methods which are popular for the experimental determination of residual stresses in materials. These methods are the layer removal method, the photoelastic (bifringence) method, and the X-Ray diffraction method.

Layer Removal Method

Srivastava and White (28) determined the residual stresses in epoxy resin sheets by the layer removal method.

This method consists of removing thin, uniform layers from a parallel-sided epoxy resin sheet. The layers are removed by the use of sandpaper or a milling machine. The imbalance of stresses in the sample will cause a curvature in the sheet. The noncontact method for measuring the curvature was by the use of laser beams and mirrors at several sites. Repeated removals and measurements developed a database of the curvature versus the depth of material removed. The residual stress is related to curvature by an equation using the material properties of the resin (28). They noted a compressive stress at the surface, and a tensile stress in the center of the sample. They found that the magnitudes of these stresses increased as the curing temperatures increased. The magnitudes of the compressive and tensile stresses encountered by Srivastava and White using the layer removal method ar comparable the to magnitudes of the compressive and tensile stresses generated by the finite element program used in this study.

Photoelastic Method

Polarized incident light is directed through a transparent and optically isotropic material in the photoelastic method of determining residual stresses. The stresses occuring in the material decompose the transmitted light into two components of different velocities which are polarized in the direction of the principal axes of the

stresses (29). An equation relates the fringe order to the principal stress difference.

The phase difference is shown as photoelastic fringes, and the fringe order, N, and the principal stress difference (o_1-o_2) are related as:

$$o_1 - o_2 = N / (\alpha * t)$$

where o_1 = a principal stress
o_2 = a principal stress
N = the fringe order
α = the photoelastic sensitivity
t = the thickness of the sample

Igarashi, et al. (29), found the maximum stress they encountered for their cured epoxy resin using the photoelastic method was 4.6 MPa. This value of 4.6 MPa encountered by Igarashi, et al. is roughly four times greater than the values of stresses generated through the finite element program.

X-Ray Diffraction Method

Diffraction methods of residual stress determination basically measure the angles at which the maximum diffracted intensity occur when a crystalline sample is irradiated with x-rays (32). The angles measured can actually be used to determine strains along various directions in the specimen and these strains are used to calculate the stresses in these directions. The X-ray diffraction can only penetrate

a thin surface layer (20 μm). Neutrons can be used to sputter the surface and allow for measurements as a function of depth.

CONCLUSIONS

An experimental study on some property effects and one-dimensional the modeling of the cure and residual stresses for thermal and electromagnetic processing of the DER 332 / DDS epoxy resin has been performed. The primary objectives in the study include experimentally determining the glass transition temperature, the thermal expansion coefficient, the Young's modulus, and the tensile strength of the cured epoxy resin resulting from both thermal and electromagnetic processing as well as developing a model which simulates the thermal and electromagnetic curing of the DER 332 / DDS epoxy resin from kinetic and heat transfer expressions. Residual stress profiles for the simulated curing of thick section epoxy resin were also determined.

The curing of thick section epoxy resins is non-uniform due to large temperature gradients in the material. The residual stresses develop due to the cooldown of the non-uniformally cured material. These stresses were evaluated at different curing temperatures and thicknesses in a thermal environment, and at different power densities and thicknesses in an electromagnetic environment.

Three steps are involved in effectively simulating the residual stresses in a material. The first step is to determine certain physical and mechanical properties as a function of the extent of cure for both thermal and electromagnetic processing. The second step is simulate the thermal and electromagnetic curing of an epoxy resin sample. The final step, the residual stress simulation, incorporates the physical and mechanical properties and the cure simulations.

A number of interesting comparisons have been made between thermal and electromagnetic processing of an epoxy resin system. The first difference encountered is the heating method used to process the sample. Thermal processing has energy transferred in through the boundaries, whereas electromagnetic processing distributes energy throughout the sample. The distribution of energy has a significant advantage in thick section samples because the thicker sample can be processed faster than the thinner sample (Figures 29,34). A thick section thermally cured sample is processed slower because conduction is the only means of transferring the energy needed to begin the reaction in the center. A significant time lag is encountered to bring thick section samples up to the reaction temperature when compared to thin samples (Figure 29). The time required to process samples with comparable

physical and mechanical properties is significantly less in an electromagnetic environment than in a thermal environment.

Two physical properties were determined as a function of the type of processing. The first property studied was the glass transition temperature of the material. The thermally processed samples had higher glass transition temperatures than the electromagnetic and combination processed samples with the equivalent extent of cure (Figure 15). The glass transition temperature is an indication of the cross-linking density in the sample. From this study, it seems that the thermal samples have a higher degree of cross-linking present than the samples electromagnetically or combination processed with the same extent of cure. The second physical property studied was the thermal expansion coefficient of the material. The samples processed electromagnetically had comparable thermal expansion coefficients to the thermally processed samples. The thermal expansion coefficient was found to be only a function of temperature in this study. The thermal expansion coefficients for the five temperature intervals are shown in Table 4.

Two mechanical properties were also determined as a function of the type of processing. The samples that were electromagnetically or combination processed had a slightly

higher Young's modulus than the thermally processed samples when plotted against the extent of cure (Figure 17). As the reaction approached completion, the modulus values for all types of processing were comparable.

The second mechanical property studied was the tensile strength of the material. The tensile strength of a sample is primarily determined by the amount of cross-linking present. The thermally cured samples had an increasing tensile strength until the extent of cure reached 80 percent and then slightly decreased as the reaction approached completion (Figure 20). The phenomena where the tensile strength is a maximum before the extent of cure reaches 100 percent is discussed in (3). The decrease in the tensile strength at the later stages of the reaction may be due to submicroscopic cracks resulting from shrinkage or thermal changes of the network segments (3). The tensile strength of the electromagnetically cured samples dramatically increased as the extent of cure increased. As the reaction approached completion, the tensile strength of the samples for all types of processing was comparable. The combination cured sample had a low tensile strength at lower curing times, however, as the the thermal portion of the cycle increased, the tensile strength of the sample also increased. For the two mechanical properties studied, the time required to produce a comparable sample in a thermal environment was twice as long as in a electromagnetic

environment.

Two cure simulations were developed which modeled the curing process of the epoxy resin system both thermally and electromagnetically. Higher curing temperatures and higher power densities resulted in samples being cured faster. Thicker samples cured slower in a thermal environment, while in an electromagnetic environment, thicker samples cured faster than thinner samples. This can be attributed to the difference in the heating methods which were discussed earlier. Large temperature gradients between the boundary and the center existed in thicker samples, as well as samples cured at higher temperatures and higher power densities. Simulated temperatures in thick section samples easily exceeded the 330 °C decomposition point.

A finite element program was used to simulate the residual stresses in samples processed thermally and electromagnetically. The residual stress simulations predict compressive stresses at the surface of the simulated sample, and tensile stresses in the center of the simulated sample (Figures 35-38). The residual stress simulations were based on the results of the extent of cure profiles developed in the thermal and electromagnetic cure simulations. Coupling the DiBennedetto equation with the extent of cure, the glass transition temperature profiles of the simulated sample were developed. The glass transition

temperature of the material determined at what temperature the residual stresses would start to develop. At temperatures above the glass transition temperature, relaxation of the molecular segment was possible and stresses could not originate. The magnitude of these stresses are increased as the cure temperature, the power density, or as the thickness of the sample is increased. These three factors all produce sample which have higher extents of cure and ultimately a higher glass transition temperature. As the reaction approached completion in the simulated sample, the magnitudes of the stresses were approaching asymptotic values. The maximum compressive stress that was encountered at the surface of the simulated sample was 1.2 MPa, and the maximum tensile stress of .75 MPa was encountered in the internal regions of the sample.

RECOMMENDATIONS

1). The thermal diffusivity was assumed to be a constant throughout the cure simulation. However, as shown in the Background and Literature Review section, the density, thermal conductivity, and heat capacity of similar resins change during the course of the reaction. These three physical properties should be modeled as a function of the temperature and of the extent of cure. These new models could be incorporated into a computer simulation program to better predict the curing cycle of thick section epoxy resin samples.

2). The electromagnetic simulation assumed a constant power input into each element of the system. The power absorbed by the system has been previously described by an equation in the Background and Literature Review section. Data for the dielectric loss factor as a function of temperature and the extent of cure has been obtained, however attempts to fit this data to a physical model has been unsuccessful. This model, along with a model for a varying power absorption, could be used to better predict an electromagnetic cure simulation.

3). The elevated temperatures found in the center of thick section materials decompose the epoxy resin. A study should be performed which evaluates the effect of the decomposition on the structural integrity of a thick section.

4). The glass transition temperature of the thermally and electromagnetically cured DER 332 / DDS epoxy resin should be studied carefully. On electromagnetically cured resin DSC thermograms, the glass transition temperature was difficult to detect. Therefore, the thermal expansion method was used to determine glass transition temperatures for these samples. However, thermally cured samples had a distinct glass transition temperature when being evaluated using DSC. The reasons for the undetectable glass transition temperature on electromagnetically cured resin DSC thermograms also should be explored.

5). A study should be performed to experimentally determine residual stresses in samples cured thermally and electromagnetically. A section has been provided in this study which describes some various methods to determine the residual stresses in materials.

6). The application of electromagnetic energy to fiber reinforced composite materials should also be studied. Preliminary experiments in a singlemode circuit have been performed on a carbon fiber / epoxy resin composite have

performed. A 24 ply composite weighing 60 grams was successfully processed using 60 watts of power for 90 minutes. The time required to electromagnetically cure this sample was significantly less than the time required to cure another comparable sample thermally. This is due to the different types of heating mechanisms found in each type of processing. It is believed that the power is absorbed along the surface of the fiber, and this will help contribute to a uniform power distribution through a thick section material.

APPENDICES

APPENDIX A

Supplementary Figures

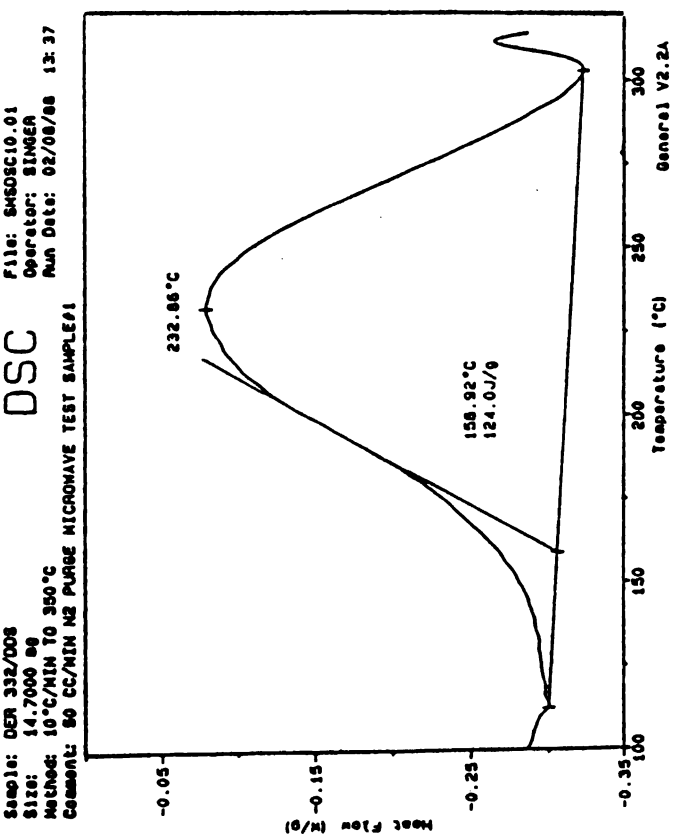

Figure 39). Example ramping DSC run at 10 °C per minute.

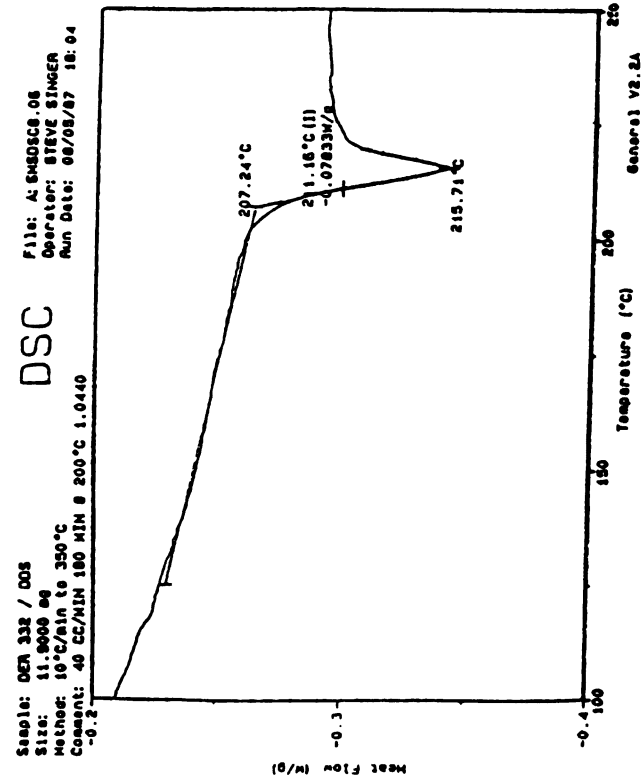

Figure 40). Example glass transition curve obtained from a run at 10 °C per minute.

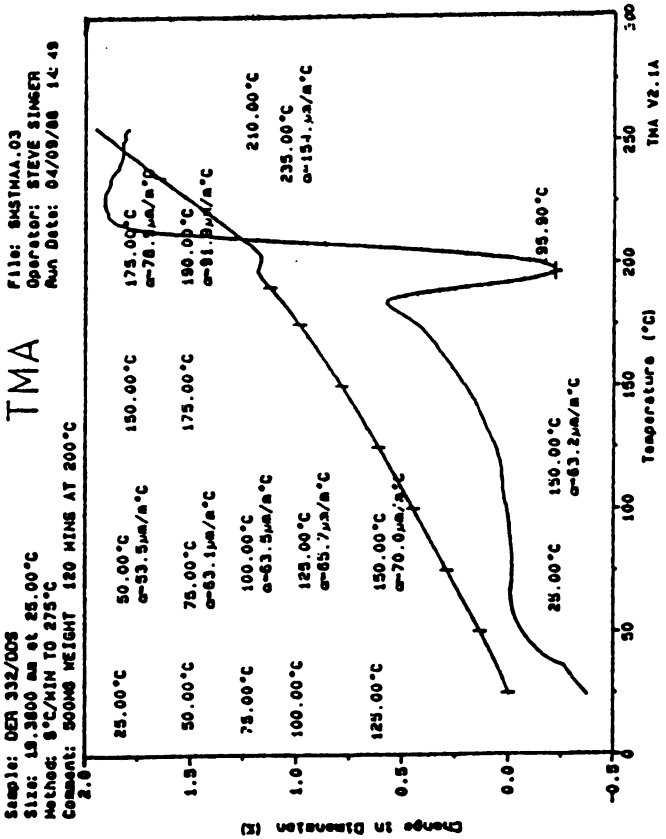

Figure 41). Example thermal expansion run at a ramping rate of 5 °C per minute.

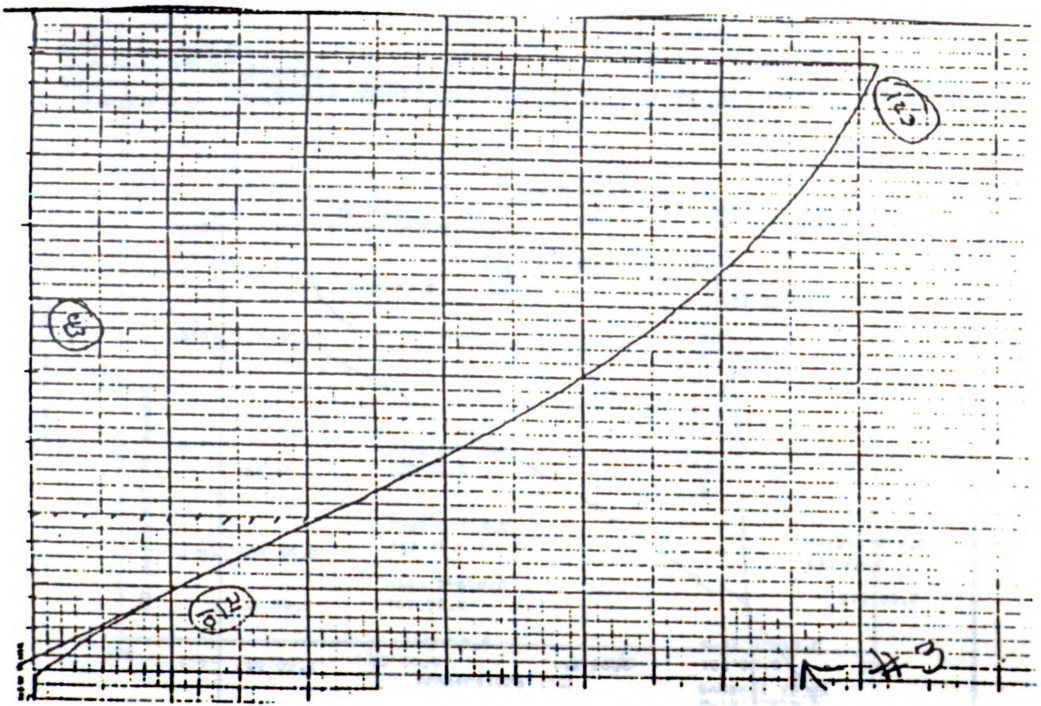

Figure 42). **Example stress-strain diagram obtained from the Instron TTC tensile testing instrument.**

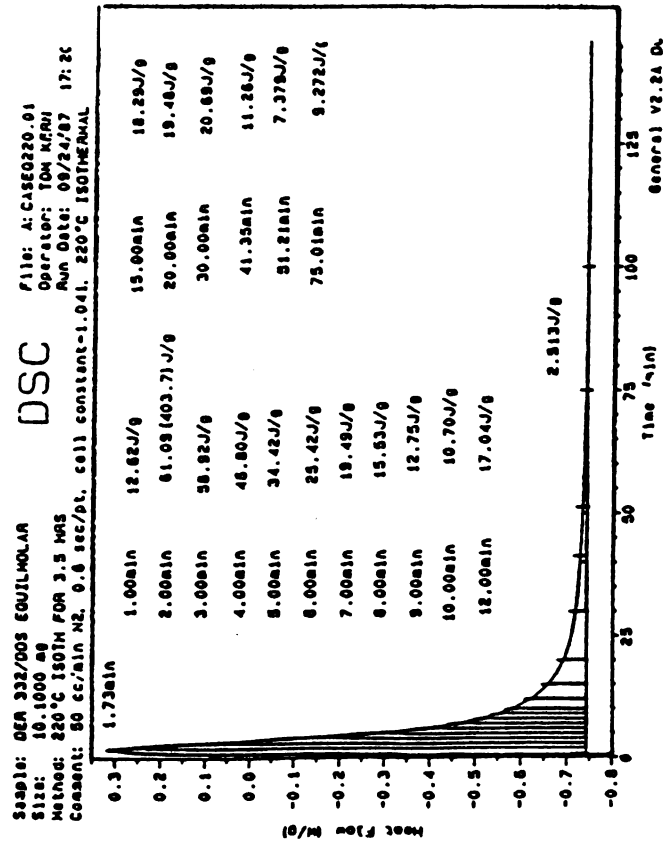

Figure 43). Example isothermal DSC run at 220 °C.

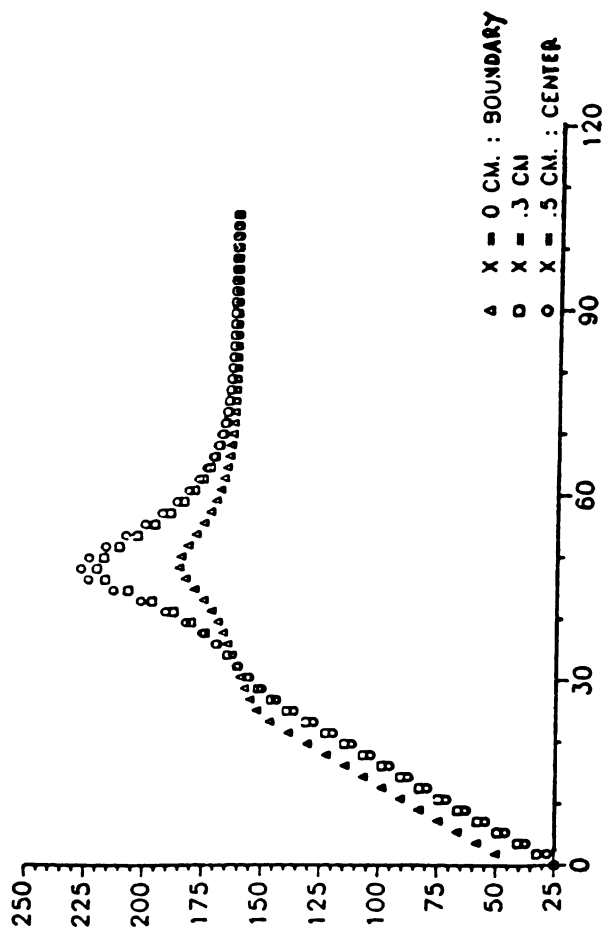

Figure 44). Simulated center temperature profiles for a one centimeter thick sample thermally cured at 160 °C.

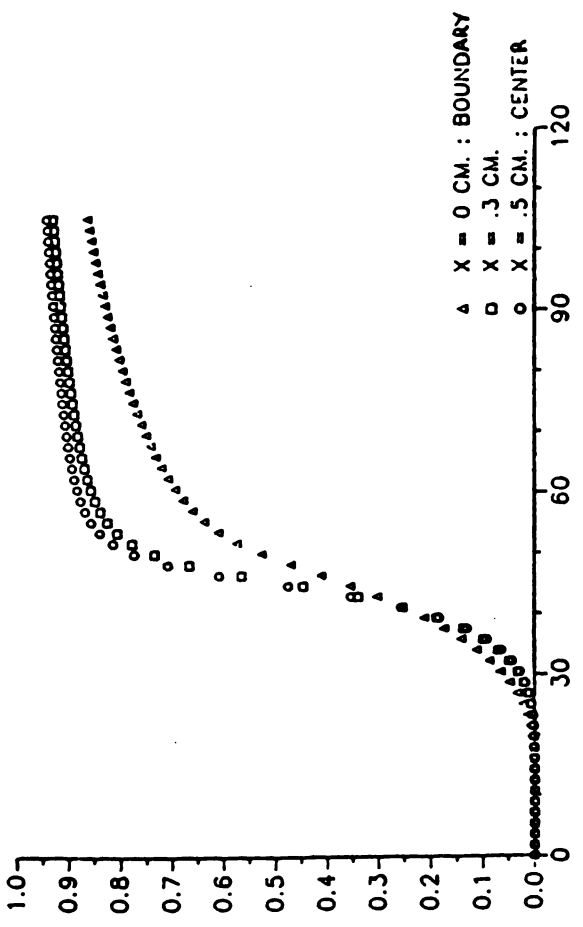

Figure 45). Simulated center extent of cure profiles for a one centimeter thick sample thermally cured at 160 °C.

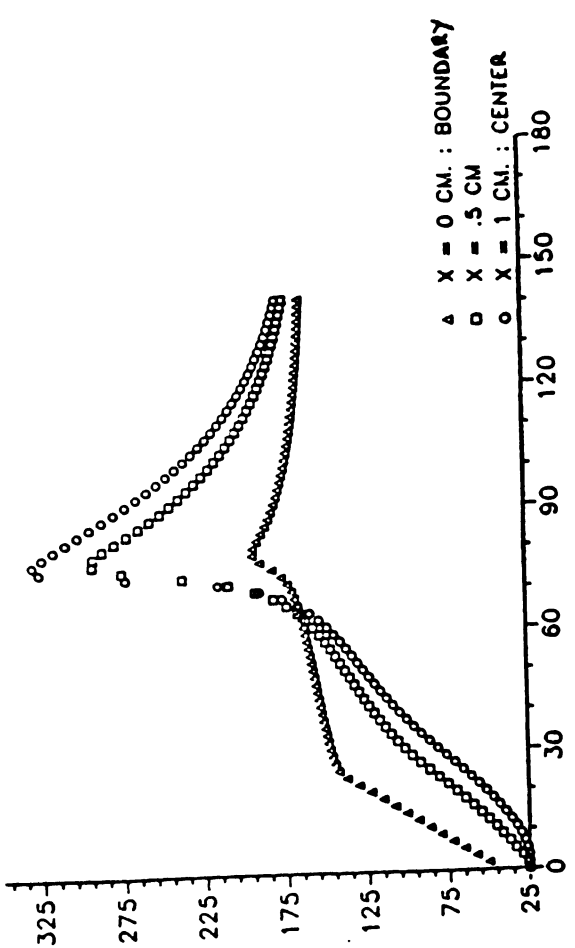

Figure 46). Simulated center temperature profiles for a two centimeter thick sample thermally cured at 160 °C.

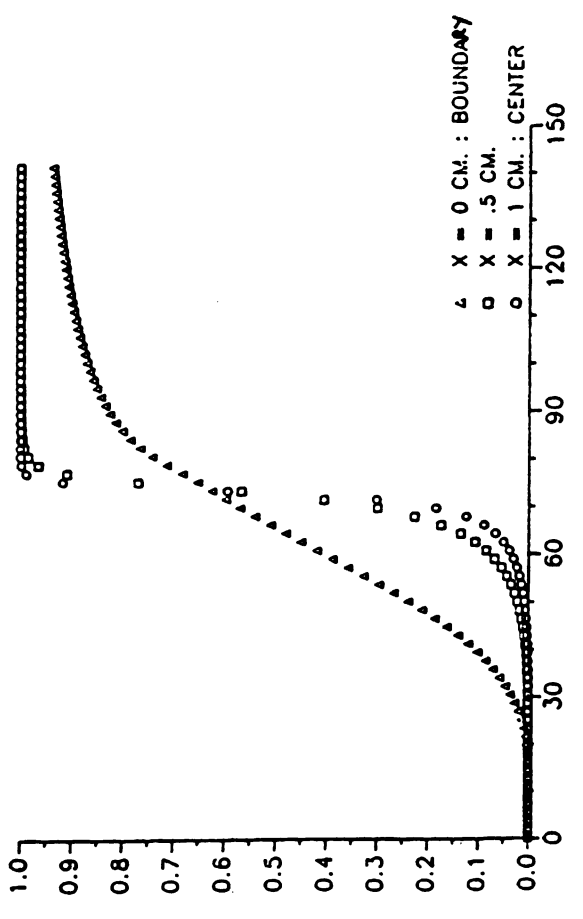

Figure 47). Simulated center extent of cure profiles for a two centimeter thick sample thermally cured at 160 °C.

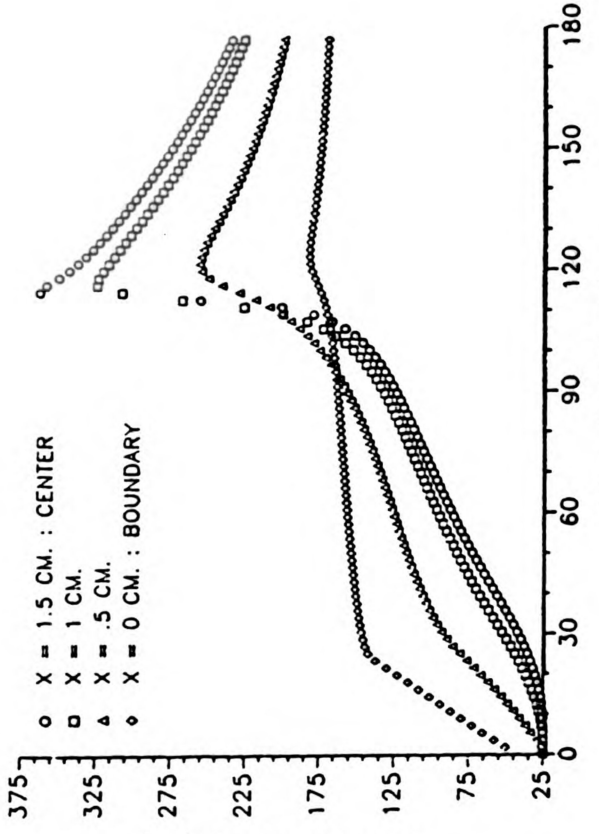

Figure 48). Simulated center temperature profiles for a three centimeter thick sample thermally cured at 160 °C.

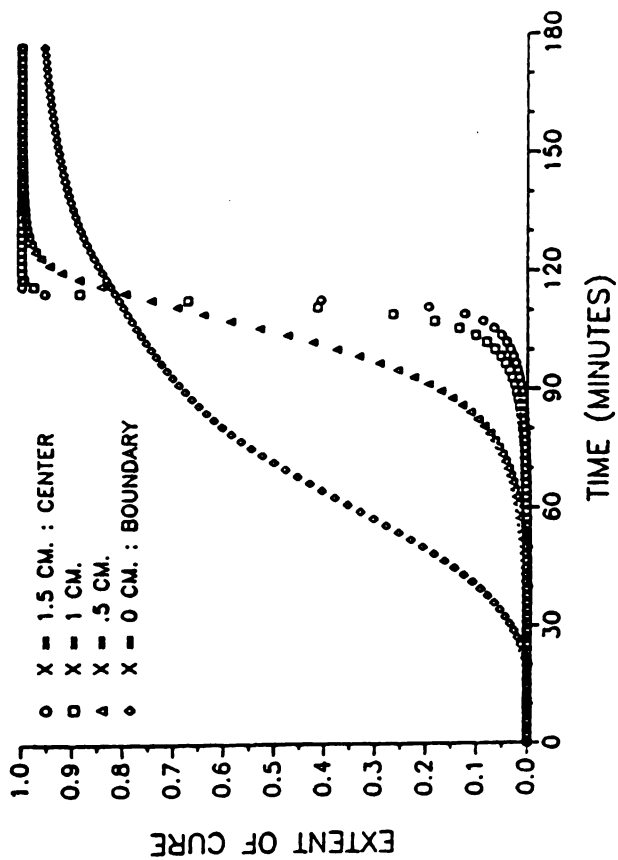

Figure 49). Simulated center extent of cure profiles for a three centimeter thick sample thermally cured at 160 °C.

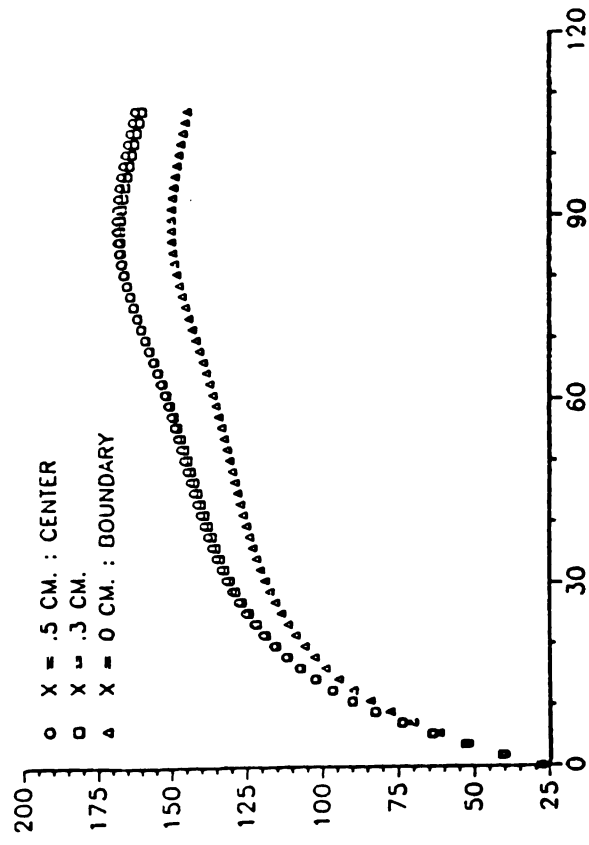

Figure 50). Simulated center temperature profiles for a one centimeter thick sample electromagnetically cured at a power density of .114 watts per gram.

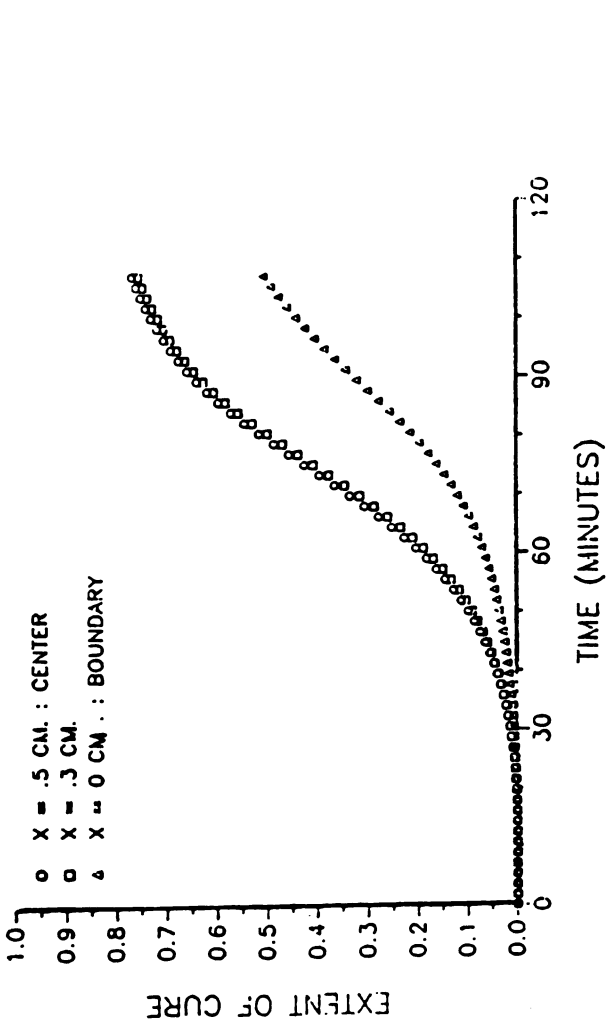

Figure 51). Simulated center extent of cure profiles for a one centimeter thick sample electromagnetically cured at a power density of .114 watts per gram.

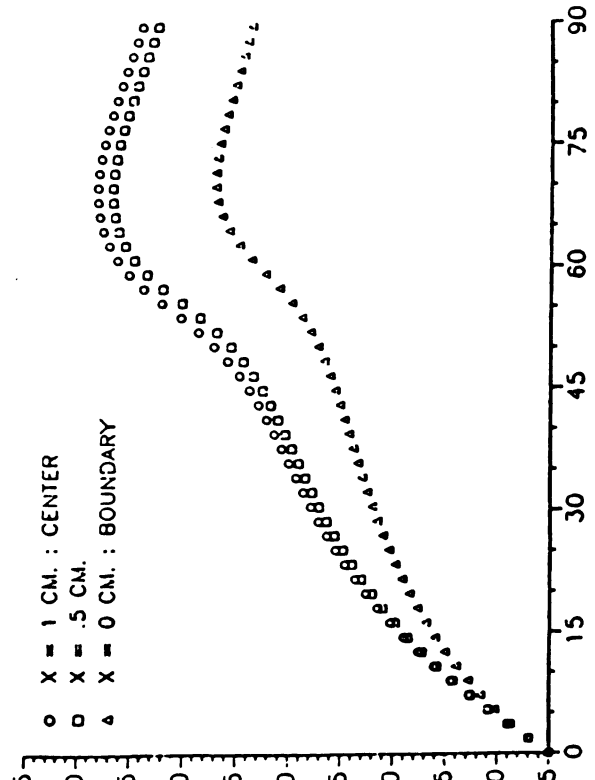

Figure 52). Simulated center temperature profiles for a two centimeter thick sample electromagnetically cured at a power density of .114 watts per gram.

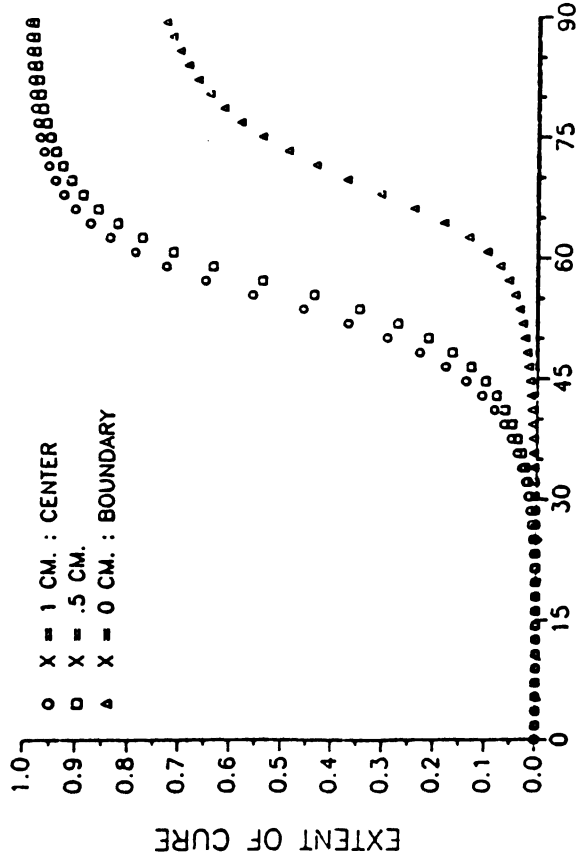

Figure 53). Simulated center extent of cure profiles for a two centimeter thick sample electromagnetically cured at a power density of .114 watts per gram.

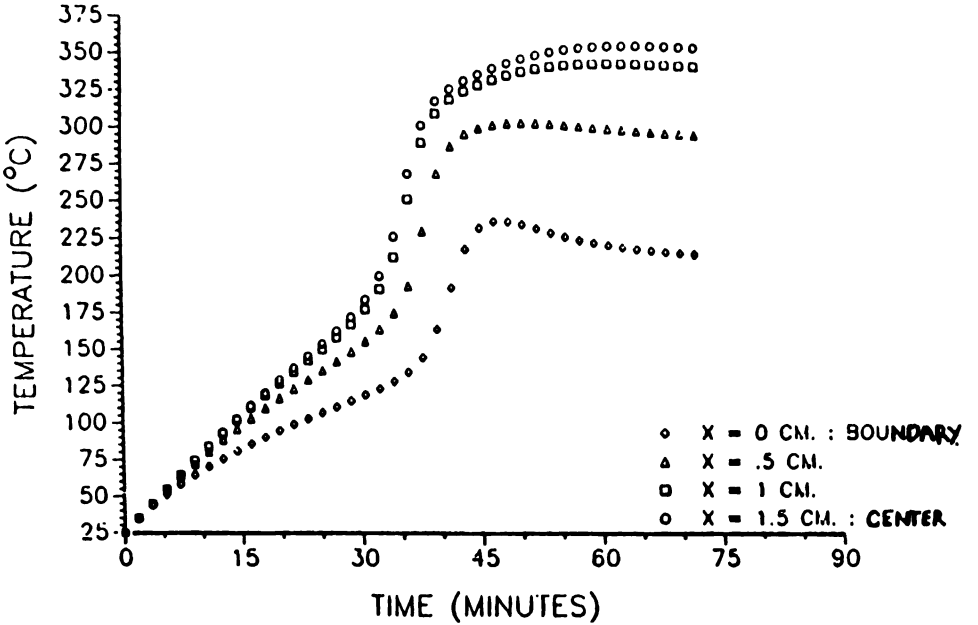

Figure 54). Simulated center temperature profiles for a three centimeter thick sample electromagnetically cured at a power density of .114 watts per gram.

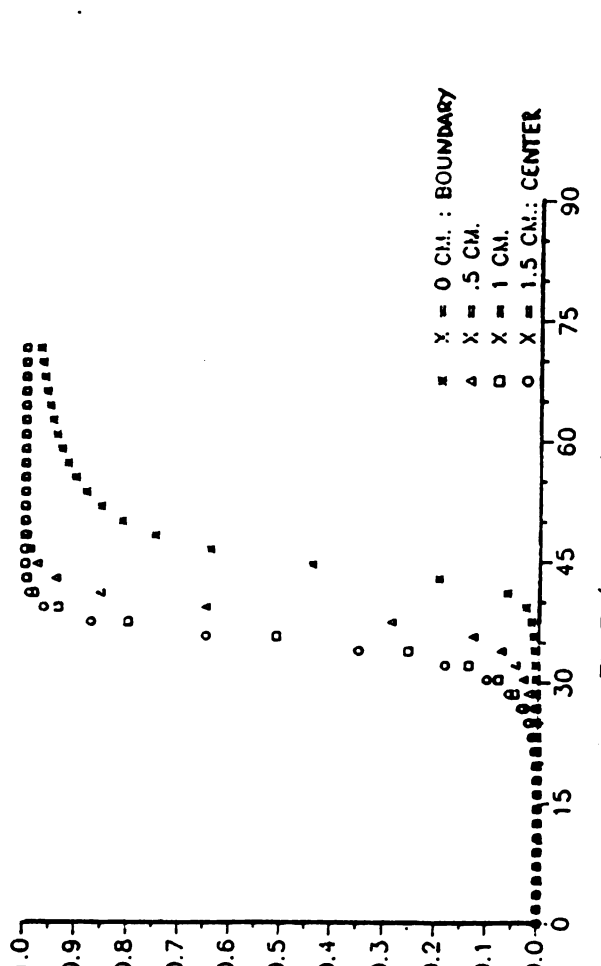

Figure 55). Simulated center extent of cure profiles for a three centimeter thick sample electromagnetically cured at a power density of .114 watts per gram.

APPENDIX B

Finite Element Method to Solve Residual Stress Problems

The finite element method can easily deal with loads or forces produced from thermal stresses. In Advanced Mechanics of Materials, Cook and Young introduce the theory of the finite element stress analysis.

The stress-strain relation for uniaxial stress is:

$$\sigma_x = E * (\epsilon_x - \alpha T)$$

where σ_x = axial force in x-direction
E = Young's modulus of the material
ϵ_x = elongation in the x-direction
α = thermal expansion coefficient
T = temperature above some uniform reference temperature

The strain-energy density U_o is:

$$U_o = \frac{E}{2} ((\epsilon_x)^2 - E\alpha T\epsilon_x)$$

The total potential is:

$$\Pi = U_o + \Omega = U_o - \sigma_x \epsilon_x$$

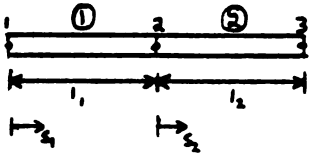

Consider a two element structure at a temperature where the structure is free of stress. If we let element 1 be cooled to an ambient temperature the total potential of the structure is:

$$\Pi = \int U_o = \int \left\{ \frac{E}{2}((\epsilon_x)^2 - E\alpha T\epsilon_x) \right\} A ds_1 + \int \frac{E}{2} (\epsilon_x)^2 A ds_2$$

The axial displacement u can be interpolated from the nodal displacements u_i and u_j by the formula:

$$u = \frac{l - s}{l} u_i + \frac{s}{l} u_j$$

Using the displacent equations we have:

$$\epsilon_x = \frac{u_2 - u_1}{l_1} \quad \text{in element 1}$$

$$\epsilon_x = \frac{u_3 - u_2}{l_2} \quad \text{in element 2}$$

Substituting the displacement equations into the total potential equation we have:

$$\Pi = \frac{AE}{2l_1} \left\{ (u_1)^2 - 2u_1u_2 + (u_2)^2 \right\} - AE\alpha T (u_2 - u_1) + \frac{AE}{2l_2} \left\{ (u_2)^2 - 2u_2u_3 + (u_3)^2 \right\}$$

The static equilibrium configuration must satisfy the following equations:

$$\frac{\delta \Pi}{\delta u_1} = 0 \qquad \frac{\delta \Pi}{\delta u_2} = 0 \qquad \frac{\delta \Pi}{\delta u_3} = 0$$

Applying the static equilibrium equations to the total potential equations and arranging in a matrix format we have:

$$\begin{bmatrix} \frac{AE}{l_1} & -\frac{AE}{l_1} & \\ -\frac{AE}{l_1} & \frac{AE}{l_1} + \frac{AE}{l_2} & -\frac{AE}{l_2} \\ & -\frac{AE}{l_2} & \frac{AE}{l_2} \end{bmatrix} \begin{Bmatrix} u_1 \\ u_2 \\ u_3 \end{Bmatrix} = \begin{Bmatrix} -AE\alpha T \\ -AE\alpha T \\ 0 \end{Bmatrix}$$

Using matrix alegbra, the displacements at the nodes can be solved. Coupling these solved displacements with the displacement equations and the stress-strain relation for uniaxial stress, the stresses in each element can be determined.

LIST OF REFERENCES

LIST OF REFERENCES

1). Goodman, S. H. ed., Handbook of Thermoset Plastics, Noyes Publications, New Jersey, 1986.

2). Turi E. ed., Thermal Characterization of Polymeric Materials, Chapter 5 "Thermosets", Prime, R.B.; Academic Press, New York, 1982, p. 435.

3). Nielsen, L. E., "Cross-Linking - Effects on the Physical Properties of Polymers", J. Macromol. Sci. - Revs. Macromol. Chem., C3(1), 1969, p. 69.

4). Bidstrup, S. A.; Sheppard, N. F., Jr.; Senturia, S. D., "Dielectric Analysis of the Cure of Thermosetting Epoxy-Amine Systems", Technical Report 8, Office of Naval Research, Contract N00014-84-K-0274, November 15, 1986.

5). Addabo, H. E.; Williams, R. J. "The Evolution of Thermosetting Polymers in a Conversion-Temperature Phase Diagram", J. Applied Science, Volume 27, 1982, p. 1327.

6). Barton, J. M., "The Application of Differential Scanning Calorimetry (DSC) to the Study of Epoxy Resin Curing Reactions", Advances in Polymer Science, Volume 72, p. 111.

7). Sichina, W. J., "Autocatalyzed Epoxy Cure Prediction Using Isothermal DSC Kinetics", DuPont Company Applications Brief Number TA-93.

8). Mijovic, J., "Cure Kinetics of Neat versus Reinforced Epoxies"; J. Applied Polymer Science, Volume 31, 1986, p. 1177.

9) Moroni, A.; Mijovic, J.; Pearce, E. M.; Foun, C. C., "Cure Kinetics of Epoxy Resins and Aromatic Diamines", J. Applied Polymer Science, Volume 32, 1986, p. 3761.

10). Hagnauer, G. L.; Pearce, P. J.; LaLiberte, B. R.; Roylance, M. E., "Cure Kinetics and Mechanical Properties of an Epoxy Matrix - Effects of Impurities and Stoichiometry", Chemorheology of Thermosetting Polymers, p. 26.

11). Jow, J., Ph.D. Thesis, Michigan State University, 1988.

12). Lewis, A.; Hedrick, J. C.; McGrath, J. E.; Ward, T. C., "The Accelerated Curing of Epoxy Resins Using Microwave Radiation", Polymer Preprints, Volume 27, No. 2, p. 330

13). Finzel, M. C., "Comparison of Multimode Microwave and Thermal Methodss for Curing Epoxy/Amine Systems", Paper presented at AICHE Conference on Emerging Technologies in Materials, August 20, 1987.

14). Strand, N. S., "Fast Microwave Curing of Thermoset Parts", Modern Plastics, October, 1980, p. 64.

15). Gourdenne, A.; Maassarani, A-H; Monchaux, P.; Aussudre, S.; Thourel, L., "Cross-Linking of Thermosetting Resins by Microwave Heating : Quantitative Approach, Polymer Preprints, Volume 20, No. 2, 1979, p. 471.

16). Gourdenne, A.; Heintz, P., "Synthesis of Interpenetrated Networks from Epoxy and Unsaturated Polyesters Using Microwave Heating", Polymer Preprints, Volume 20, No. 2, 1979, p. 388.

17). Wilson and Salerno "Microwave Curing of Epoxy Resins", U. S. Army Aviation Research and Development Command, Contract # DAAG46-76-C-0035, September, 1978.

18). Mijovic, J.; Wang, H. T., "Modeling of Processing of Composites Part II - Temperature Distribution during Cure", SAMPE Journal, March / April 1988, p. 42.

19). Shimbo, M.; Ochi, M.; Shigeta, Y., "Shrinkage and Internal Stress during Curing of Epoxide Resins", J. Applied Science, Volume 26, 1981, p. 2265.

20). Bruins, P. F. ed., Epoxy Resin Technology, Chapter 4, "Commercial Epoxy Resin Curing Agents", Perez, R. J., Interscience Publishers, New York, 1968.

21). Bruins, P. F. ed., Epoxy Resin Technology, Chapter 1, "General Chemistry of Bisphenol A-Based Resins", Dowd, R. T., Interscience Publishers, New York, 1968.

22). Gupta, V. B.; Drzal, L. T.; Lee, C. Y-C.; Rich, M. J., "The Temperature Dependence of Some Mechanical Properties of

a Cured Epoxy Resin System", Polymer Engineering and Science, Volume 25, No. 13, 1985, p. 812.

23). Adamson, M. J., "Thermal Expansion and Swelling of Cured Epoxy Resin Used in Graphite/Epoxy Composite Materials", J. Material Science, Volume 15, 1980, p. 1736.

24). Morgan, R. J., "Structure-Property Relations of Epoxies Used as Composite Matrices", Advances in Polymer Science, Volume 72, p. 1.

25). Enns, J. B.; Gillham, J. K., "Effect of the Extent of Cure on the Modulus, Glass Transition, Water Absorption, and the Density of an Amine-Cured Epoxy", J. Applied Science, Volume 28, 1983, p. 2831.

26). Browning, C. E. ed., Composite Materials: Quality Assurance and Processing, ASTM 797, Kardos, J. L.; Dudukovic, M. P.; McKague, E. L.; Lehman, M. W., "Void Formation and Transport During Composite Laminate Processing: An Initial Model Framework", Philadelphia, 1983, p. 96.

27). Loos, A. C.; Springer, G. S., "Curing of Epoxy Matrix Composites", Journal of Composite Materials, Volume 17, March 1983, p. 135.

28). Srivastava, A. K.; White, J. R., "Curing Stresses in an Epoxy Polymer", J. Applied Science, Volume 29, 1984, p. 2155.

29). Igarashi, T.; Kondo, S.; Kurokawa, M., "Contractive Stress of Epoxy Resin during Isothermal Curing", Polymer, Volume 30, 1979, p. 301.

30). Tsai, S. W.; Hahn, H. T., Introduction to Composite Materials, Technomic Publishing Company, Connecticut, 1980.

31). Fritz, R., Personal Communication

32). Noyan, I. C.; Cohen, J. B., Residual Stress - Measurement by Diffraction and Interpretation, Springer Verlag, New York, 1987.

33). Cook, R. D.; Young, W. C., Advanced Mechanics of Materials, Macmillan Publishing Company, New York, 1985.

34). Treuting, R. G.; Wishart, H. B.; Lynch, J. J.; Richards, D. G, Residual Stress Measurements, American Society of Metals, Cleveland, 1952.